Plant Molecular Biology (2023) 112:119–142
https://doi.org/10.1007/s11103-023-01342-8

Comparative transcriptome sequencing analysis to postulate the scheme of regulated leaf coloration in *Perilla frutescens*

Xiaoning Liu[1] · Yanning Zhai[1] · Jingyu Liu[1,2] · Jingqi Xue[1] · Tatjana Markovic[3] · Shunli Wang[1] · Xiuxin Zhang[1]

Received: 10 August 2022 / Accepted: 17 February 2023 / Published online: 8 May 2023

Abstract

Perilla as herb, ornamental, oil and edible plant is widely used in East Asia. Until now, the mechanism of regulated leaf coloration is still unclear. In this study, four different kinds of leaf colors were used to measure pigment contents and do transcriptome sequence to postulate the mechanism of leaf coloration. The measurements of chlorophyll, carotenoid, flavonoid, and anthocyanin showed that higher contents of all the aforementioned four pigments were in full purple leaf 'M357', and they may be determined front and back leaf color formation with purple. Meanwhile, the content of anthocyanin was controlled back leaf coloration. The chromatic aberration analysis and correlative analysis between different pigments and *L*a*b** values analysis also suggested front and back leaf color change was correlated with the above four pigments. The genes involved in leaf coloration were identified through transcriptome sequence. The expression levels of chlorophyll synthesis and degradation related genes, carotenoid synthesis related genes and anthocyanin synthesis genes showed up-/down-regulated expression in different color leaves and were consistent of accumulation of these pigments. It was suggested that they were the candidate genes regulated perilla leaf color formation, and genes including *F3'H*, *F3H*, *F3',5'H*, *DFR*, and *ANS* are probably important for regulating both front and back leaf purple formation. Transcription factors involved in anthocyanin accumulation, and regulating leaf coloration were also identified. Finally, the probable scheme of regulated both full green and full purple leaf coloration and back leaf coloration was postulated.

Key message

The contents of pigments determined front and back leaf coloration, and the key regulated gene were identified, and the probable scheme of regulated front and back leaf coloration was postulated.

Keywords Perilla · Leaf color · Chlorophyll · Carotenoid · Anthocyanin · Transcriptome sequencing

Xiaoning Liu, Yanning Zhai and Jingyu Liu have contributed equally to this work.

✉ Shunli Wang
wangshunli@caas.cn

✉ Xiuxin Zhang
zhangxiuxin@caas.cn

Xiaoning Liu
lxn731125@163.com

Yanning Zhai
zhaiyanning@caas.cn

Jingyu Liu
liujingyu981226@163.com

Jingqi Xue
xuejingqi@caas.cn

Tatjana Markovic
tmarkovic@mocbilja.rs

[1] Key Laboratory of Biology and Genetic Improvement of Flower Crops (North China)Ministry of Agriculture and Rural Affairs, China, Institute of Vegetables and Flowers, Chinese Academy of Agricultural Sciences, Beijing 100081, China

[2] College of Landscape and Forestry, Qingdao Agricultural University, Qingdao 266109, China

[3] Nstitute for Medicinal Plants Research "Dr Josif Pancic", 11000 Belgrade, Serbia

Introduction

Perilla frutescens (L.) Britton as an herbaceous plant belongs to Lamiaceae family, and is widely cultivated throughout several Asian countries (Gaihre et al. 2021; Nakajima et al. 2015; Wang et al. 2020a, b). Now, it has been an economic crop and a source of medicine and spices in China, Korea, Japan, and other many countries (Tong et al. 2015). This species includes two cultivated types, viz. *P. frutescens* var. *frutescens*, and *P. frutescens* var. *crispa* according to their morphology and uses, and they have being freely cross-fertile with each other by artificial pollination. In China and Korea, *P. frutescens* var. *frutescens* with green leaf is an important oil crop and also used as vegetable crops in Korea, while *P. frutescens* var. *crispa* with purple leaf extensively cultivated in China and Japan, are more often used for medicinal properties, fish garnish and ingredient for various foods (Gaihre et al. 2021; Tong et al. 2015).

Leaf color variations are large in perilla, and therefore it is also used as an ornamental plant (Zhang et al. 2021). Perilla leaves contain many bioactive components including phenolic compounds, rosmarinic acid, caffeic acid, flavanone, anthocyanin, vitamins, amino acids, polysaccharides, and minerals (Nakajima et al. 2015; Deguchi and Ito 2020; Miki et al. 2015; Zheng et al. 2020). These compounds have various pharmacological activities, such as anti-oxidative activity, anti-inflammatory, anti-anxiety, anti-cancer activities, anti-depressive activities, and beneficial for gastrointestinal digestion (Wang et al. 2020a, b; Zheng et al. 2020; Kwak and Ju 2015). In addition, perilla is one of the plant species with the most abundant α-linolenic acid (Zhang et al. 2021). As traditional Chinese medicine, *P. frutescens* has been widely used in treating colds, coughs, vomiting, constipation, and food poisoning in clinical settings (Nakajima et al. 2015; Wang et al. 2020a, b; Kwak and Ju 2015). Recently, it was found that perilla leave extracts had ability of inhibiting severe acute respiratory syndrome coronavirus (SARS-CoV-2) replication by inactivating the virion (Tang et al. 2021). Previous studies showed that purple perilla leaves have high anti-oxidative activities than that of green perilla leaves due to the different concentrations of anthocyanins and flavonoids (Zheng et al. 2020). Therefore, deciphering the molecular mechanism of leaf coloration is benefit for exploring perilla function.

Metabolomics, differential display of mRNA, and transcriptome technology have been used to investigate green and red leaf coloration and a few regulated genes of leaf coloration have been identified in *P. frutescens* (Yamazaki et al. 2003, 2008). The regulation of anthocyanin (mainly malonylshisonin) production, but not that of other metabolites determined the red and green forma (Yamazaki et al. 2003). The key enzymes of anthocyanin synthesis including *glutathione S-transferase* (*PfGST1*) and *chalcone isomerase* (*PfCHI*) were preferentially expressed in the leaf of red perilla (Yamazaki et al. 2008). Tong et al. (2015) used RNA-seq sequenced four samples, including one weedy and one cultivar of var. *frutescens*, and two cultivars of varieties *crispa* with red and green leave color of *Perilla*. According to expression profiling between *P. frutescens* (L.) var. *frutescens* and var. *crispa*, 22, 962 differently expressed genes (DEGs) were detected in the weedy variety compared to the cultivars, 18 unigenes assigned to anthocyanin played important roles in determining leaf color were identified (Tong et al. 2015). A total of 77 unigenes involved in flavonoid biosynthesis were identified in purple and green perilla leaf by transcriptomic approaches, and highly expressed *chalcone isomerase* (*PfCHS*) enhanced accumulation of red perilla leaf (Zhang 2021). However, back leaf coloration is still unclear. The other key genes regulated leaf color, such as transcription factor genes, should be further identified for deciphering molecular mechanisms of perilla leaf color formation.

Chlorophyll, carotenoids and anthocyanins are the primary pigments that determine plant leaf color. In fact, the leaf color variations of perilla are extensive, and the leaf color contains green, red, purple, light purple, dark purple and etc.. Much more studies were focused on anthocyanins, but not considering chlorophyll, carotenoid, and other pigment change, together. The mechanism of leaf color formation should be further studied.

In this paper, four different perilla cultivars with four kinds of leaf colors were used as materials. The leaves of four cultivars in their strong growth stage were collected for pigment measurements and transcriptome sequencing. The photosynthesis rate and color aberration were also tested. The correlation between pigment content and leaf color change were analyzed, and key genes and related regulatory genes controlled leaf color formation were also obtained. The probable scheme of regulated both green and purple leaf color formation and back leaf coloration was postulated at last.

Materials and methods

Plant materials and sample collection

One cultivar '94' from *P. frutescens* var. *frutescens* and three cultivars including '272', '103' and 'M357' from *P. frutescens* var. *crispa* were used as material in this work. The front and back leaf color were different in these four cultivars and their leaf colors were shown in Fig. 1. The front and back leaf colors of '94' and 'M357' were completely green and completely purple, respectively. In '272', the leaf color was front green and back light purple, while

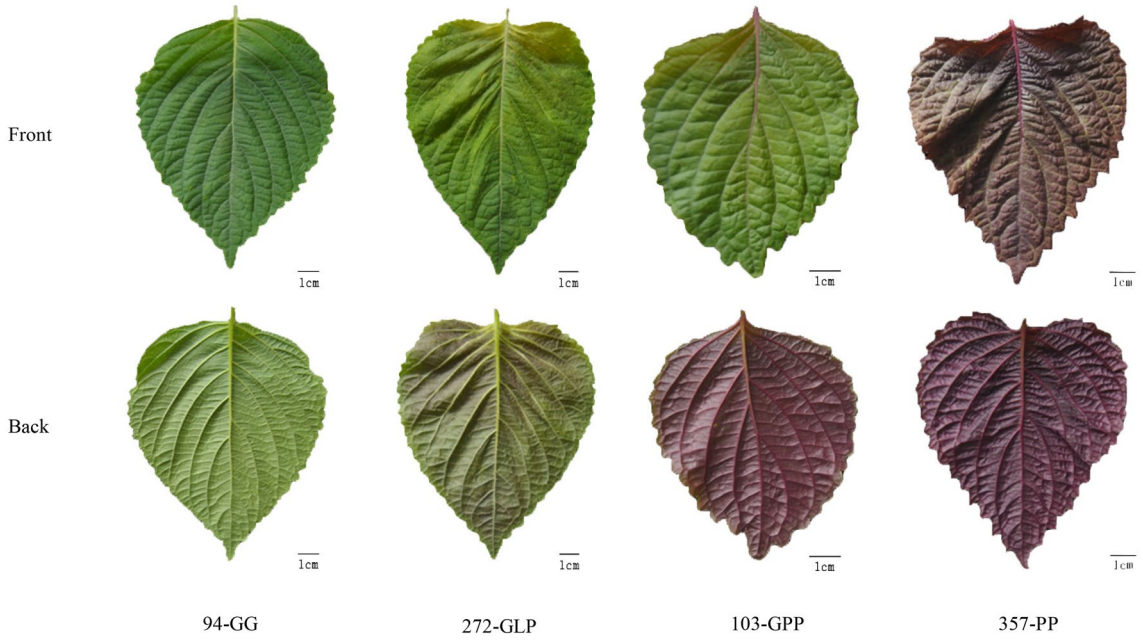

Fig. 1 The morphology and the front and back leaf color of four cultivars '94', '272', '103', and 'M357'

the leaf color of '103' was front green with purplish vein at bottom and back dark purple (Fig. 1). 94-GG, 272-GLP, 103-GPP, and 357-PP were represented cultivars '94', '272', '103', and 'M375' and their color abbreviation, respectively. The same abbreviations are used below in this work. The perilla seeds were introduced from Oil Crops Research Institute, Chinese Academy of Agricultural Sciences (CAAS), Wuhan city, Hubei Province, China, and Guizhou Academy of Agricultural Science, Guizhou city, Guizhou Province. After seedling culture, the two leaves' stage seedlings were transplanted in the experimental field of the Institute of Vegetables and Flowers, CAAS in Beijing, China, on 20th-April-2021. The leaves in strong growth stage were collected on 6th-June-2021. In this stage, the leaf colors of the four cultivars have been steadily formed. The fresh leaves were immediately frozen in liquid nitrogen, and stored in a refrigerator at − 80 °C until use. Other two developmental leaf stages including original leaf color, and middle leaf color of the '272' and '103' were also collected on for chromatic parameters analysis on 1st-June-2021 and 3rd-June-2021, respectively.

Measurements of chlorophyll, carotenoid, anthocyanin, and flavonoid content

The pigment content was determined using a 722 spectrophotometer (Shanghai Jinghua Technology Instrument Co., Ltd, Shanghai, China) after extraction with 80% acetone. Concentration of Chl *a*, Chl *b*, Chl (*a* + *b*), and carotenoids in the obtained extracts was calculated according to the formulas (Ivanov et al. 2020).

The total anthocyanin content of leave extract was determined using a modified pH differential method according to previous reports in Rabino and Mancinelli (1986). The anthocyanin of leaf was extracted at 4 °C in acidic (1% HCl, w/v) methanol for 48 h. The absorbance of the supernatant was determined at 520 nm and 700 nm using a 722 spectrophotometer (Shanghai Jinghua Technology Instrument Co., Ltd, Shanghai, China) at pH 1.0 and 4.5 conditions with modified by HCl, respectively. The total anthocyanins content were calculated according Eqs. 1, and 2, respectively. For comparison purposes, pigment content was calculated as cyanidin 3-glucoside using an extinction coefficient (ε) of 29,600 L mol^{-1} cm^{-1} and molecular weight of anthocyanins 449.2. Measurements were replicated four times with means being reported.

$$\text{Absorbance (A)} = \left(A_{520} - -A_{700}\right)\text{pH1.0} - \left(A_{520} - -A_{700}\right)\text{pH4.5} \quad (1)$$

$$\text{Anthocyanin (mg/L)} = A \times Mw \times DF \times 10^3/(\varepsilon \times L). \quad (2)$$

Mw is the molecular weight of anthocyanins (449.2 g/mol), DF is the dilution factor, ε is the extinction coefficient (29,600 L mol^{-1} cm^{-1}), and L is the path length (1 cm).

The measurement of flavonoid content was referred to previous report (Matvieieva et al. 2019). Each sample was measured in triplicate.

Photosynthetic measurements of four perilla cultivars

The photosynthesis of four perilla cultivars were measured at 9:30 am–10:00 am during three continuous sunny days from 6th-June-2021 to 8th-June-2021, using portable photosynthesis system (CRAS-3, Lufthansa Technology Group, Beijing, China) that maintains photosynthetic photon flux density at 1,200 μmol m^{-2} s^{-1} and CO_2 concentration at 400 μmol mol^{-1}. Four photosynthetic parameters, namely net photosynthetic rate (P_n) estimated by CO_2 uptake (it is also represented by "A" in the equipment), stomatal conductance (gs; it is also represented by "gsw" in the equipment), intercellular CO_2 concentration (C_i), and transpiration rate (T_r; it is also represented by "E" in the equipment). The procedures were performed by manufacture of company. The three mature leaves of each plant were used for all above measurements, with three biological replicated for each samples.

Analysis of leaf chromatic aberration

The front and back leaves were measured with a hand-held color analyser (CM-2500D, Konica Minolta, Japan) in the room, according to the CIE *L*a*b** system. The leaf colors were expressed as three main colors parameters, including *L**, *a** and *b** value (McGuire 2019; Voss 1992). The color coordinate *L** represents lightness, from black (0) to white (100), *a** describes red (positive) to green (negative), and *b** describes yellow (positive) to blue (negative). Chroma (C*) can be calculated based on the equations $C^* = (a^{*2} + b^{*2})^{1/2}$, and hue angle (*h*) were calculated using the formulae $h = \tan^{-1}$ (b*/a*). The experimental materials were collected from at least three plants and three points on each leave were measured.

RNA extraction, construction of the cDNA library, and transcriptome sequencing

Total RNA was isolated from fresh leaves of four perilla cultivars using a Trizol extraction kit (Invitrogen, USA), according to the instructions of the manufacturer. The concentration and integrity of RNA per sample was determined using an Agilent Bioanalyzer 2100 (Agilent Technologies, Santa Clara, CA, USA), and the quality of RNA was measured using a NanoDrop 2000 UV/Visible spectrophotometer (Thermo Scientific™, USA). The mRNA enrichment and cDNA library construction were referred to previous reports (Wang et al. 2019; Gao et al. 2020). A total of eight RNA-seq libraries (two libraries for each sample) were constructed and then sequenced using an Illumina HiSeq™4000 (4 × 100 bp read length) platform at the Beijing Genomics Institute Company (Shenzhen, China). All obtained data are available at the NCBI Short Read Archive and the accession number is and SRP371629.

De novo transcriptome assembly and functional annotation

The clean reads were produced by removing the reads contained adapters, unknown nucleotides (Ns), low quality reads (phred score < 20), and terminal nucleotides in both 3' and 5' ends, as well as relatively short reads (< 50 nt) from the raw reads (Lohse et al. 2012). The high-quality clean reads were de novo assembled using Trinity software to construct unique consensus sequences (Grabherr et al. 2011).

All assembled unigenes were annotated in the following six databases: NCBI non-redundant protein database (NR), NCBI non-redundant nucleic acid sequence database (NT), Swiss-Prot protein sequence database (Swiss-Prot), Gene Ontology (GO), Kyoto Encyclopedia of Genes and Genomes (KEGG), and Clusters of EuKaryotic Orthologous Groups (KOG) using BLAST software (Altschul et al. 1990). Blast2GO was used to perform GO annotation (Conesa et al. 2005). The potential coding sequencing (CDS) of unigenes identification and the simple sequence repeats (SSRs) prediction was used the program TransDecoder and MISA software (http://pgrc.ipk-gatersleben.de/misa/), respectively.

Differentially expressed genes (DEGs) identification, and GO and KEGG enrichment

The expression levels of genes were calculated using fragments per kilobase of exon region per million mapped reads (FPKM) values. The FPKM value for each gene was determined based on the length of the gene and reads count mapped to this gene. The unigenes showed differential expression levels among different samples were calculated based on the ration of FPKM values. Meanwhile, the differently expressed genes (DEGs) were evaluated based on the genes with FPKM of > 1 in at least one sample. The DEGs between any two comparisons were identified using DEseq2, and Benjamini and Yekutieli's method was used to adjust the resulting *P*-values, to minimize the false detection rate (FDR) (Benjamini and Yekutieli, 2005). A false discovery rate (FDR) ≤ 0.001, *Q*-values ≤ 0.05, *P*-values ≤ 0.001 and the absolute value of |log2(Fold change)| ≥ 1 were used as the thresholds to determine the significance of the gene expression differences. Furthermore, the DEGs were subjected to Gene Ontology (GO) and KEGG pathway classification and functional enrichment analysis s. The hierarchical clustering of DEGs was constructed by Mev software (Wang et al. 2020a, b).

Validation of gene expression by quantitative real-time PCR (qRT-PCR)

A total of 14 interested DEGs related to chlorophyll and anthocyanins metabolisms were randomly selected to validate the expression levels through quantitative real-time PCR (qRT-PCR). The total RNA extraction, mRNA purification, cDNA synthesis, and qRT-PCR reaction were conducted according to Wang et al., (2012). The *actin* gene was selected as a reference gene (Jiang et al. 2020). The primers used in qRT-PCR are summarized in Table S1. All qRT-PCR reactions were carried out in triplicate using independent samples.

Statistical analysis

All the results in the experiment were repeated at least three times. The experimental data are expressed as mean ± the standard error (SE) and were conducted using one-way ANOVA, followed by Duncan's multiple range tests at $p < 0.05$ level. The statistical significance among leaves with different colors was performed with the SPSS 22.0 (SPSS Institute, IBM, Endicott, NY, USA).

Results

Pigment levels in four perilla cultivars

The transplanted seedlings grew well in the experimental field and the front and back leave colors of '94' and 'M357' kept steady with green and purple color, respectively, in all the growth stage (Fig. 1). The cultivar '272' and '103' underwent quick color changes, and then the leaf colors were steady in all growth stage (Fig. 1). Finally, the back of mature leaf in '272' and '103' turned light and dark purple, respectively. At same time, the front leaf color of '272' was still green, and the front leaf color was green with light purplish vein at the bottom of leaf in '103'.

For chlorophyll and carotenoid contents, it was found notable difference among four cultivars. The total chlorophyll and carotenoid contents of 357-PP were highest among the four cultivars (Fig. 2A). For anthocyanin, the largest content was also in 357-PP, followed by 103-GPP, and the low contents were in 94-GG and 272-GLP (Fig. 2B). The anthocyanin content was around 20 fold higher in 357-PP than that of in 272-GLP (Fig. 2B). The total content of flavonoid was also high in 357-PP (Fig. 2C).

Analysis of photosynthetic parameters in four perilla cultivars

Four photosynthetic parameters were shown in Fig. 3. For the net photosynthetic rate, 357-PP had highest level, followed by 103-GPP, and the lowest level was in 272-GLP. Concerning the G_s, it was closely matched the P_n curve and the highest level was in 357-PP. Similarly, the T_r and G_s curves had the same trends of P_n. According to the chlorophyll contents of four cultivars, perilla cultivar with higher chlorophyll contents has higher photosynthetic rate.

Identification of leave color in four perilla cultivars

The chromatic parameters of the front and back leaves of each samples were recorded using the CIE *L*a*b** color system (Table 1). The values of *L*a*b** of original leaf colors of 272-GLP, and 103-GPP were similar with those in 94-GG (Table 1). After leaf color steady, the values of *a* b** in the front leaf colors were ranged from − 15.81 to 4.79, and 4.55 to 22.77, respectively, while they were ranged from − 14.12 to 8.76, and 2.19 to 22.16, respectively, in the back leaf colors (Table 1). The *a** represents red and green color. The values of the chromatic parameters *a** in 357-PP was distinct from those in other three cultivars, because it showed positive *a** values (mean 4.79) in the front leaf and lowest (mean 2.19) among four perilla cultivars in back leaves. The *L** values (mean 40.28, 48.86 in front and back, respectively) of the front and back leaves were high in

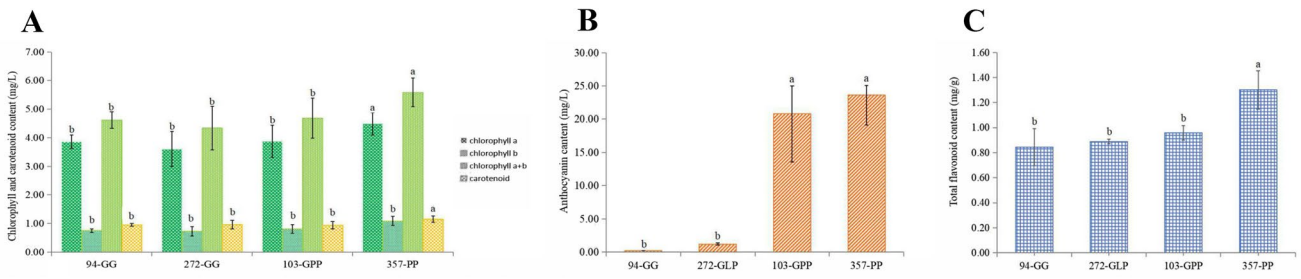

Fig. 2 The contents of chlorophyll and carotenoid (**A**), anthocyanin (**B**), and total flavonoid (**C**) in different colored leaves of four perilla cultivars. 94-GG, 272-GLP, 103-GPP, and 357-PP were represented cultivar '94', '272', '103', and 'No.375', and their leaf color abbreviation, respectively. The same abbreviations are used below. a, b, and c indicate significant differences at the $P < 0.05$ level

green leaves of '94', and low in front leave of 'M357' (mean 25.56) and back leave of 'No.101' (mean 27.21) and 'M357' (28.45). These samples show no significant differences in hue (Table 1). The lowest chroma value (*C**) was in 6.61. As described, these measured results were consistent with the leaf pigmentation appearance.

The correlative analysis between pigment contents and the *L***a***b** values in front leaf showed that chlorophyll, carotenoid, anthocyanin, and flavonoid were positive

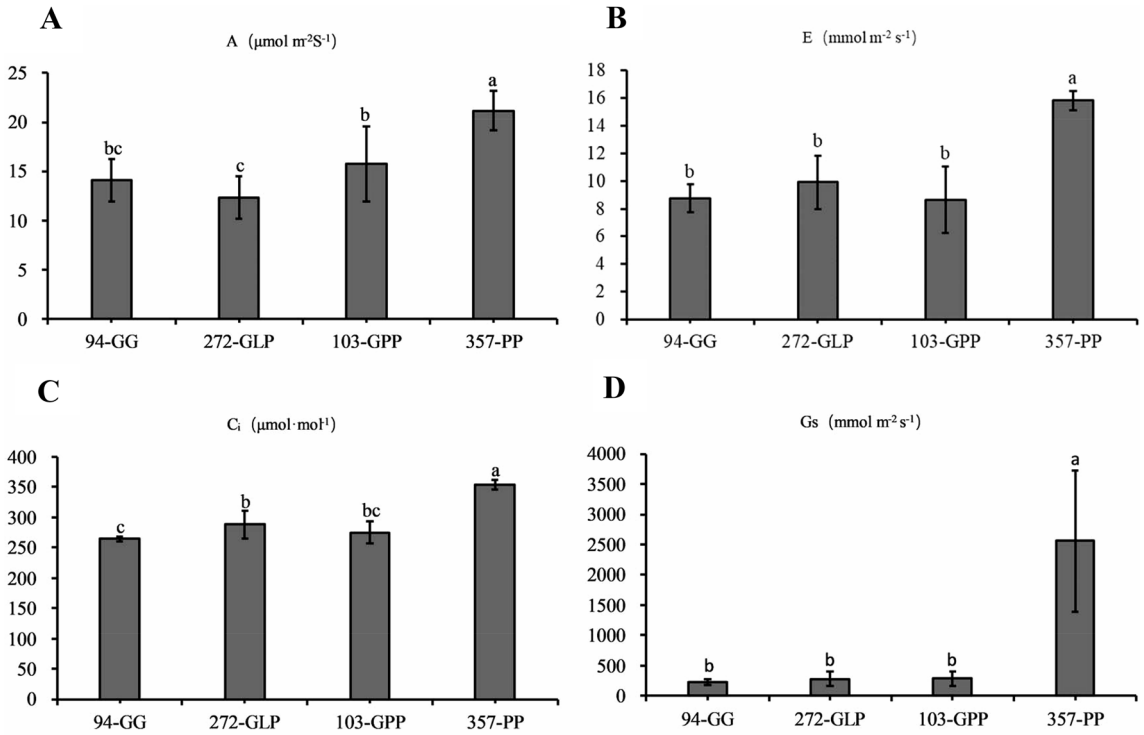

Fig. 3 The comparison of net photosynthetic rate (P_n/A) (**A**), transpiration rate (Tr/E) (**B**), intercellular CO_2 concentration (C_i) (**C**), and stomatal conductance (G_s) (D) among four perilla cultivars

Table 1 The CIE *L***a***b**chromatic parameters in front and back leaf of four perilla cultivars

Cultivars	Front leaf					Back leaf				
	*L**	*a**	*b**	*C**	h^c	*L**	*a**	*b**	*C**	h^c
94-GG	40.28	− 15.81	22.77	27.72	− 0.96	48.86	− 14.12	22.16	26.28	− 1.00
272-GLP	36.43	− 13.58	20.34	24.46	− 0.98	36.42	− 1.27	11.12	11.19	− 1.46
103-GPP	35.23	− 11.93	18.93	22.38	− 1.01	27.21	8.43	3.16	9.00	0.36
357-PP	25.56	4.79	4.55	6.61	0.76	28.45	8.76	2.19	9.03	0.24
272-orignal	39.86	− 17.06	26.65	31.64	− 1.00	45.59	− 12.97	20.57	24.32	− 1.01
272-middle	37.12	− 14.02	22.22	26.27	− 1.01	40.25	− 6.97	15.33	16.84	− 1.14
103-orginal	40.32	− 13.24	21.07	24.88	− 1.01	47.64	− 11.30	19.78	22.78	− 1.05
103-middle	34.09	− 11.82	16.58	20.36	− 0.95	34.90	2.35	7.07	7.45	1.25

Table 2 The correlative analysis between different pigment contents and *L***a***b** values of front and back leaf

Pigment	*L** (front)	*a** (front)	*b** (front)	*L** (back)	*a** (back)	*b** (back)
Chlorophyll	− 0.562	0.593	− 0.656*	− 0.735**	0.800**	− 0.714*
Carotenoid	− 0.499*	0.616**	− 0.559*	− 0.101	0.202	− 0.180
Anthocyanin	− 0.892**	0.889**	− 0.889**	− 0.471	0.505	− 0.520
Flavonoid	− 0.525*	0.609**	− 0.548*	− 0.145	0.183	− 0.215

related to a^* value, and they together determined purple leaf color formation (Table 2). In back leaf, only anthocyanin and flavonoid has positive correlative relationship with a^* value (Table 2). It was indicated that back leaf color change was controlled by anthocyanin.

Tri-dimenstional graphics allowed evidencing that separation among the four leaf color types. The front leaf color analysis showed that 357-PP in one room, while the other cultivars in the same room. The original color of 272-GLP and 103-GPP and 94-GG was close in the same room, while the colors of their middle stage were close to their steady colors (Fig. 4A). For the back leaf color analysis, purple leaf of 103-GPP and 357-PP were in the same room and steady color of 272-GLP and color of middle stage in 103-GPP was in other room (Fig. 4B). As a whole, for 272-GLP and 103-GPP, the front leaf colors were relatively steady, and their back leaf colors were gradually change during growth and steady at last (Fig. 4).

Illumina sequencing and de novo transcriptome assembly

In this work, 51.43 Gb nucleotides were produced by Illumina sequencing BGISEQ platform. After the removal of adapter sequences, ambiguous reads and low quality reads, total of 42.86 Gb clean reads were assembled into 128,041 unigenes, with average sequence length of 1,488 bp (Table S2). The N50 length, N90 length, and GC percentage of assembled unigenes were 2,229 bp, 807 bp, and 40.93%, respectively (Table S2). The top three sequence length distribution and percentage of the unigenes were 200–300 bp (15.04%), 300–400 bp (6.74%), and 400–500 bp (4.57%), respectively (Fig. S1A). A total of 13,714 unigenes were longer than 3000 bp (10.71%) (Fig. S1A). These results showed that the quality of sequencing data was good. BUSCO quality evaluation also showed assembled unigenes were complete and reliable, and complete(C) and single-copy(S) of all unigenes arrived at 96 (Fig. S1B). A total of 78,105 protein coding sequences (CDS) with 84,896,910 bp total length were detected using Transdecoder, and the 300–400 bp CDS (11.96%) were highly aligned (Fig. S2, Table S3). The maximum CDS length reached to 15,303 bp, and a total of 2,201 CDS were longer than 3000 bp (2.82%) (Table S3).

Functional annotation of perilla leaf transcriptomes

The assembled unigenes were annotated to seven public databases, including nonredundant protein sequence database (Nr), nucleotide sequence database (Nt), Swiss-prot (Swissprot), Kyoto encyclopedia of genes and genomes (KEGG), clusters of orthologous groups of proteins (KOG/COG), Pfam, and gene ontology (GO). In total, 98,086 unigenes (76.61%) could be annotated in at least on database, while there were 37,219 unigenes (29.07%) successfully annotated in all seven databases (Fig. 5; Table 3). The venn diagram of Nr, Nt, Swissprot, KEGG, and GO database showed that 44,972 unigenes were annotated in all the five public databases (Fig. 5A). The species showed the best BlastX matches were *Sesamum indicum* which took up 45.39%, the second- and third-ranked species *Handroanthus impetiginosus* and *Erythranthe guttata* was contributed to 22.38%, and 12.87%, respectively (Fig. 5B). For GO assignments, 69,508 unigenes matched to Nr database were further divided into 38 major functional groups. Of all the GO term categories, binding (34,680), membrane part (20,741), and cellular process (14,769) were the highest ranking in the three GO categories molecular function, cellular component, and biological process, respectively (Fig. 5C). A total of 74,907 unigenes were mapped to KEGG pathways, and global and overview maps (15,265, 20.38%), carbohydrate

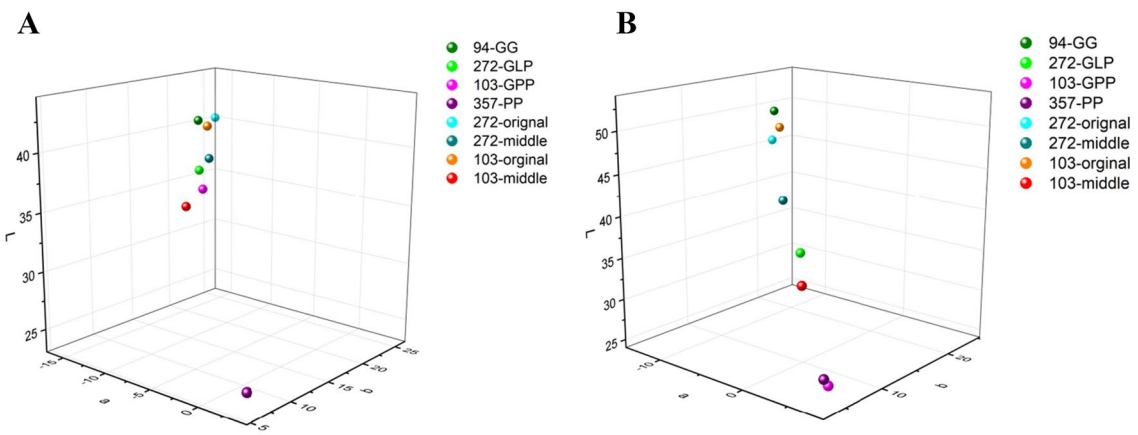

Fig. 4 The distribution of chromatic coordinates of front (**A**) and back (**B**) leaf in four perilla cultivars

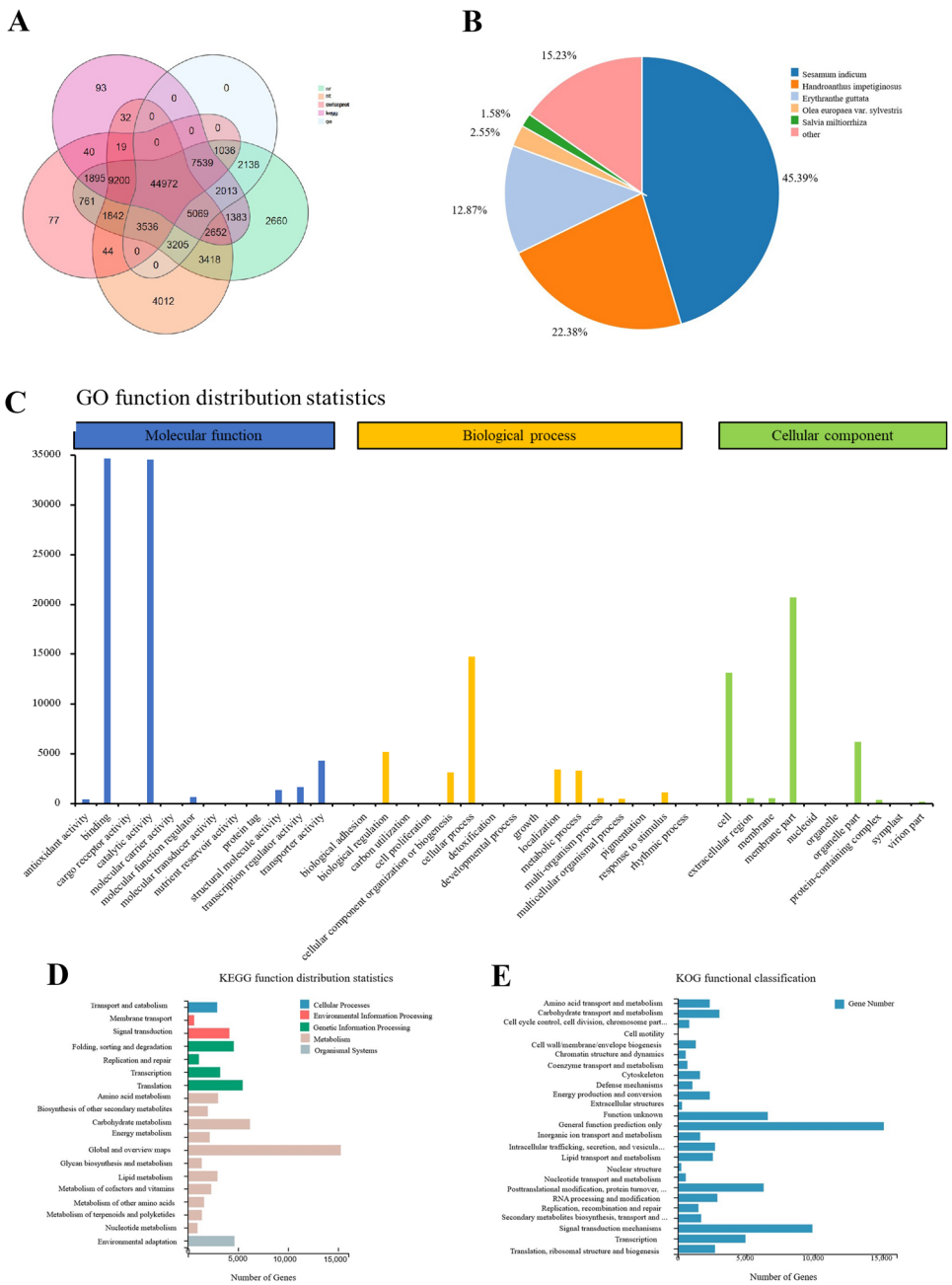

Fig. 5 Venn diagrams of the five public databases annotation including Nr, Nt, Swissprot, GO, and KEGG (**A**), Species distribution (**B**), Gene Ontology (GO) assignments (**C**), KEGG pathways distribution (**D**), and KOG functional classification (**E**) for perilla transcriptome unigenes

Table 3 The annotations of perilla leaf unigenes against the seven public databases

Values	Total	NR	NT	SwissProt	KEGG	KOG	Pfam	GO	Intersection	Overall
Number	128,041	93,319	78,001	70,961	74,907	73,203	71,543	69,508	37,219	98,086
Percentage	100%	72.88%	60.92%	55.42%	58.50%	57.17%	55.88%	54.29%	29.07%	76.61%

metabolism (6,206, 8.28%), and translation (5,472, 7.31%) were occupied the top three ranking (Fig. 5D). The 73,203 unigenes were classified into 25 KOG classifications. General function prediction only (15,060, 20.57%) had the most representation, followed by signal transduction mechanisms (9,836, 13.44%) and function unknown (6,570, 8.98%) (Fig. 5E).

Gene structure analysis suggested that 3,577 simple sequence repeats (SSRs) were detected in 26,807 unigenes (Fig. S3A). In addition, 3,577 transcript factors

were predicted in this study (Fig. S3B) Principle components analysis (PCA) showed that four cultivars were clustered different positions and purple leaf 'M357' was apart from the other three perilla cultivars (Fig. S4A). Gene expression profiles of accumulative bar diagram composite column-diagram showed that many unigenes (FPKM values = 1–10) were distributed in M357-PP (Fig. S4B). These results indicated that transcriptome sequencing could be used to identify the leave color regulated genes in perilla. A total of 78,700 unigenes were expressed in all the four cultivars were seen in Fig. S4C.

Analysis of differentially expressed genes (DEGs) with different pairwise comparisons

In order to explore the differentially expressed genes (DEGs) among four perilla cultivars with different leaf colors, the gene expression levels between each pairwise comparison were studied, and then DEGs were identified by different pairwise comparisons (Fig. S5; Fig. S6). The highest number of DEGs was appeared in 272-GLP versus 357-PP (35,381) among six pairwise comparisons, with 17,824 and 17,577 unigenes up- and down-regulated, respectively (Fig. S5). In contrast, the lowest number of DEGs was observed in 272-GLP versus 103-GPP (19,376), with 13,369 and 12,088 unigenes up- and down-regulated, respectively (Fig. S5). The venn diagrams of any three pairwise comparison showed that highest number of DEGs (9,670) were common to the 357-PP versus 94-GG, 357-PP versus 272-GLP and 357-PP versus 103-GPP comparisons, and the lowest number of DEGs were common in 94-GG versus 103-GPP, 103-GPP versus 272-GLP and 94-GG versus 272-GLP comparisons (Fig. S6A-D). Furthermore, much more DEGs (1,795) were observed in many purple leaf attended pairwise comparisons including 357-PP versus 94-GG, 357-PP versus 103-GPP, 103-GPP versus 272-GLP and 357-PP versus 272-GLP than those pairwise comparisons with many green leaf attended comparisons, '94-GG versus 272-GLP', '94-GG versus 357-PP', '94-GG versus 103-GPP' and 103-GPP versus 272-GLP (Fig. S6E-F). A total of 611 DEGs were common to the 357-PP versus 94-GG, 357-PP versus 103-GPP, 357-PP versus 272-GLP, 94-GG versus 272-GLP, and 94-GG versus 103-GPP comparisons (Fig. S6G). These results suggested that the genes regulated green and purple color had more significant difference. Notably, many DEGs were appeared in the pairwise comparisons contained purple leaf of 357-PP.

GO functional and KEGG pathway enrichment of DEGs and their expression patterns analysis

GO functional enrichment analysis of DEGs revealed that of top three main enrichment of the GO among five comparisons viz. 357-PP versus 94-GG, 357-PP versus 103-GPP, 357-PP versus 272-GLP, 94-GG versus 103-GPP, and 103-GPP versus 272-GLP, were ribosome (GO:0005840), and translation (GO:0006412) and structural constituent of ribosome (GO:0003735), respectively (Fig. S7). In 94-GG versus 272-GLP, the top three ranking GO functional enrichment were ADP binding (GO:0043531), photosystem I (GO:0009522), and photosynthesis, light harvesting (GO:0009765), respectively (Fig. S7E). The GO functional enrichment further analysis showed that the categories of photosynthesis (GO:0015979), chloroplast thylakoid membrane (GO:0009535), photosystem I (GO:0009522), and II (GO:0009523), chloroplast (GO:0009507), were all enriched among the above six pairwise comparisons. The categories of photosystem I reaction center (GO:0009538), and L-phenylalanine catabolic process (GO:0006559) were specifically distributed in 357-PP versus 103-GPP. We also found the GO functional enrichment of pairwise comparisons with green leaf cultivar was different with those with purple leaf cultivar. These results were also suggested that the content, synthesis and metabolim of chlorophyll, and photosynthesis ability were different in four perilla cultivars with different leave colors.

A total of 50 DEGs related to photosystem I and II, photosynthesis, light harvesting, chloroplast thylakoid membrane, chlorophyll binding, chloroplast, chloroplast envelope, photosynthesis, photosystem I reaction center, ferredoxin-NADP + reductase activity and PS II associated light-harvesting complex II catabolic process, and photosynthesis were identified and summarized in Table S4.

It is interested that the DEGs enriched in photosynthesis, light harvesting in photosystem I, such as *chlorophyll a/b-binding protein* genes (CL125.Contig9_All, Unigene136_All, Unigene127_All, Unigene128_All) and photosystem I reaction center, *photosystem I reaction center subunit* genes (CL10496.Contig2_All, CL5429.Contig4_All, CL238.Contig4_All, CL12334.Contig1_All, and CL13338.Contig3_All) showed up-regulated expression pattern in 357-PP (Table S4). These results suggested that purple leaf of perillia have strong ability of light harvesting and photosynthesis in photosystem I, compared with those of green or green plus purple leaves. However, ferredoxin-NADP + reductase activity related genes showed down-regulated expression pattern in purple leaves. The key gene controlled chlorophyll synthesis, such as *magnesium-chelatase subunit ChlD* (Unigene12797_All) *CPO* (CL5607.Contig4_All, CL2268.Contig3_All), *PPOX* (CL3522.Contig4_All, CL1474.Contig27_All), and *MgCh* (CL9498.Contig1_All), showed up-regulated in 94-GG and 103-GPP. At the same time, the gene *chlorophyll M* (*CHLM*, Unigene17397_All), *chlorophyll 27* (*CHL27*, CL1169.Contig13_All), and *protochlorophyllide reductase* (*POR*, CL374.Contig6_All) control chlorophyll synthesis were also up-regulated in 357-PP, while the *Chlorophyll synthase* (*CHLG*, CL5824.Contig3_All) were

down-regulated in 357-PP. However, the *MCS/SGR/NYC1* (CL5222.Contig3_All, CL3099.Contig4_All, CL3287.Contig1_All, CL3709.Contig1_All, CL6196.Contig1_All, and CL3865.Contig1_All), with *PPH* unigenes (Unigene19598_All and Unigene19603_All), and *pheophorbide a oxygenase* (*PAO*) (CL9496.Contig2_All) played role in chlorophyll degradation was down- and up-regulated, respectively, in 357-PP. In chlorophyll recycling process, chlorophyll *a* and *b* could not be easily recycling in purple leaf 357-PP, according to lower expression of *CAO* (CL1364.Contig13_All), *CBR* (CL3043.Contig4_All), and *HCAR* (CL6020.Contig12_All) (Fig. S8A). As a whole, it was deduced that more chlorophyll synthesis in green leaf, while the chlorophyll degradation rate was slow at the beginning, and then fast in purple leaf 357-PP.

In chloroplast enrichment, *zeaxanthin epoxidase* (*ZEP*, CL950.Contig28_All) regulated carotenoid synthesis also showed up-regulated expression in 357-PP (Fig. S8B, Table S4). It was suggested that carotenoid may be played in leaf color formation.

KEGG pathway enrichment analyses of DEGs with $p < 0.001$ as the threshold were also performed in six pairwise comparisons. Like GO functional enrichment, 94-GG versus 272-GLP had a little difference with other five pairwise comparisons. In 357-PP versus 94-GG, 357-PP versus 272-GLP, and 357-PP versus 103-GPP comparisons, the top one to five ranking pathways all include ribosome (ko03010), carbon fixation in photosynthetic organisms (ko00710), photosynthesis-antenna proteins (ko00196), and photosynthesis (ko00195), flavonoid biosynthesis (ko00941, ranked sixth in 357-PP versus 94-GG) (Fig. S9A-C). Notably, porphyin and chlorophyll metabolism (ko00860) in 357-PP versus 94-GG was ranked fifth, and it was also enriched in 357-PP versus 272-GLP, and 357-PP versus 103-GPP (Fig. S9A). It was further suggested that chlorophyll metabolism was different among four cultivars with four kinds of leaf colors. Phenylpropaniod biosynthesis (ko00940), stilbenoid, diarylheptanoid and gingerol biosynthesis (ko00945) were also common in the above three pairwise comparisons. In 94-GG versus 272-GLP, 94-GG versus 103-GPP, and 103-GPP versus 272-GLP comparisons, carbon fixation in photosynthetic organisms (ko00710), photosynthesis (ko00195), porphyin and chlorophyll metabolism (ko00860), photosynthesis-antenna proteins (ko00196), phenylpropaniod biosynthesis (ko00940), and flavonoid biosynthesis (ko00941) were common in these three comparisons (Fig. S9D-F). Flavone and flavonol biosynthesis (ko00944), and isoflavonoid biosynthesis (ko00943) were specific observed in 357-PP versus 94-GG and 94-GG versus 272-GLP, and 357-PP versus 103-GPP, respectively comparisons.

A total of 17 DEGs related to carotenoid biosynthesis (ko00906) were also identified in five pairwise comparisons (Fig. S8B, Table S4). The DEGs including *9-cis epoxycarotenoid dioxygenase* (*NCED*, Unigene214_All), *carotenoid cleavage dioxygenase* (*CCD7*, CL14084.Contig2_All), and *zeaxanthin epoxidase* (CL950.Contig28_All), showed much more expression in purple leaf, compared with those in green leaf. The up-regulation of *beta-carotene isomerase D27* (*DWRF27*, Unigene32590_All), *phytoene synthase 2* (*PSY2*, CL6263.Contig2_All), *cytochrome P450 CYP97A41* (*CYP97A41*, CL12610.Contig3_All), *15-cis-zeta-carotene isomerase* (*ZIISO*, CL3672.Contig2_All), and *cytochrome P450 CYP97A41* (CL12610.Contig3_All) was showed in green leaf (Fig. 8B). The kinds of carotenoids were different in purple leaf 357-PP and in green leaf 94-GG, according to these genes' expression. It was deduced that the neoxanthin and carlactone, and lutein were highly accumulated in purple leaf 357-PP and in green leaf 94-GG, respectively.

The DEGs enriched by KEGG pathway related to chlorophyll metabolism, flavonoid biosynthesis, and photosynthesis were analyzed and summarized in Table S4. Most of DEGs enriched photosynthesis, porphyrin and chlorophyll metabolism (ko00860), and photosynthesis—antenna proteins (ko00196) were same as those DEGs in GO functional enrichment. Especially, chlorophyll breakdown gene *MCS/SGR/NYC1* (CL5222.Contig3_All, CL3099.Contig4_All and CL3709.Contig1_All) highly expressed in 94-GG suggested fast chlorophyll degradation was in green leaf.

A total of 13 and 24 DEGs related to phenylpropanoid biosynthesis (ko00940), and flavonoid biosynthesis (ko00941) were screened out in KEGG enrichment, respectively. They were took part in perilla leaf color formation. The *PAL* (CL13983.Contig3_All), *C4H* (Unigene27773_All, Unigene14839_All, CL6772.Contig2_All), *C3H* (CL11971.Contig9_All) *HCT* (CL13936.Contig3_All, Unigene10775_All, and Unigene5083_All) and *COMT* (Unigene17835_All) all showed up-down expression pattern in 94-GG, 272-GLP, 103-GPP and 357-PP (Fig. 8C, Table S4). Much more expression of *PAL*, *C4H*, *C3H*, and *HCT* would be caused much more caffeic acid synthesis in green and front green and back purple leaves in 94-GG, 272-GLP, and 103-PP, compared with that of only purple leaf 357-PP. Much more caffeic acid synthesis might be promoted rosomarinic acid synthesis. *Rosomarinic acid synthesis* gene, *RAS* (CL13662.Contig2_All) also showed high expression in 272-GLP and 94-GG (Fig. 8C; Table S4). Many *CCR* (CL14054.Contig2_All, CL1293.Contig1_All), *4CL* (CL12689.Contig5_All, Unigene15858_All, Unigene9488_All, and CL3950.Contig8_All) unigenes showed up-regulation in purple cultivar 'M357'. At the same time, the key anthocyanins synthesized genes *CHS* (Unigene15383_All) and *CHI* (CL3453.Contig1_All) all highly expressed in 357-PP.

As a whole, the genes related to flavonoid 3'-hydroxylase (F3'H), flavonoid 3',5'-methyltransferase-like (F3',5'H), dihydroflavonol 4-reductase (DFR), and anthocyanidin

synthase/leucoanthocyanidin dioxygenase (LODX/ANS) showed specific expression in 103-GPP and 357-PP. Highly expressed of these above genes induced much more anthocyanins accumulation. Much more expression of F3',5'H gene could be promoted delphinidin-3-glycoside accumulation and further cause leaf of 357-PP turning purple (Fig. 8C). Based on F3'H, F3H, and FSII gene expression, it was suggested that much more flavones, flavonals, and isoflavones might synthesized in green leaf, compared with that in the purple leaf (Fig. 8C, Table S4).

The hierarchical clustering analysis of key DEGs involved in chlorophyll metabolism and flavonoid biosynthesis

According to the results of venn diagrams and DEGs enriched GO function and KEGG pathway (Fig. S4, Fig. S9), all the genes referred to chlorophyll biosynthesis and metabolisms were searched. Meanwhile, the expression patterns of these genes according to FPKM of RNA-seq data in four perilla cultivars were analyzed, and the relationship between their expression patterns and leaf color formation was investigated. The 23 chlorophyll synthesis and degradation related genes (59 unigenes or contigs) were identified in our work (Table 4). For this study, without those genes with a FPKM value of less than 1, a total of 55 unigenes or contigs were different expressed and probably related to leaf color formation. The hierarchical clustering thermogram of 55 DEGs was shown in Fig. 6A. The different four cultivars could be easily separated by expression levels of 42 unigenes, and it was indicated that these genes may be regulated leaf coloration.

At the same time, the 20 flavonoid synthesis related genes were also analyzed according to different pairwise comparisons with different groups, and a total of 102 unigenes or contigs were identified (Table 5). Without those genes with a FPKM value of less than 1, the remaining 73 unigenes or contigs were different expressed in four perilla cultivars and they were probably related to perilla leaf color formation. Their hierarchical clustering thermogram was shown in Fig. 6B. According to heatmap cluster, the relationship of cultivar 272 and 94, and 103 and 357 was close, respectively (Fig. 6B). It was suggested that these flavonoid synthesis related genes were regulated perilla leaf color.

The important transcription factor genes involved in perilla leaf color regulation

Transcription factors (TFs) play an important role in plant development and secondary metabolism. In this paper, a total of 28 TF genes were identified and they have different expression patterns in four perilla cultivars. It includes one AP10/EREBP gene, one bZIP gene, one MADS box gene *SVP*, one TCP gene, four MYB gene, one zf-HD gene, two NAC21/22 genes, three WRKY genes, four WD40 genes, and seven bHLH genes. The AP10/EREBP, bHLH35-like, bHLH29, bHLH137-like, bZIP, SVP, MYB-like, MYB113, NAC21/22, WD40 repeat containing protein 23, U4/U6 small nuclear ribonucleoprotein PRP4-like protein, and autophagy-related protein 18b were up-regulated and the remained 14 TFs were down-regulated (Fig. 7, Table 6). The relationship of four cultivars constructed by heatmap was similar with that constructed by flavonoid. It was suggested that these TFs might control flavonoid accumulation, and effect leaf color formation. The bHLH35-like (CL1476.Contig1_All), and WD repeat-containing protein 43 (CL4426.Contig1_All) and zinc-finger homeodomain protein 3 (CL13045.Contig26_All) were specifically expressed in 272-GLP and 103-GPP, respectively. Previous study showed that *MYB113* regulated perilla leaf color, and this TF was also identified in our work. Meanwhile, *MYB61* (CL3951.Contig1_All) and MYB-like (CL12881.Contig13_All) showed same expression pattern as *MYB113* viz. up-regulated in deep color leaves. TF genes including *AP10/EREBP* (CL1914.Contig26_All), *bZIP* (CL403.Contig9_All), *SVP* (CL11571.Contig4_All), *NAC21/22* (Unigene3776_All and Unigene4273_All), and *bHLH137-like* (Unigene631) also highly expressed in purple leaf 357-PP (Fig. 7B). It was suggested that these TFs may regulated perilla leaf color formation.

Validation of candidate DEGs by qRT-PCR

In order to further verify the reliability of the RNA-Seq data, 14 genes from the DEGs related to the flavonoid synthesis and cholophyll metabolism were randomly selected, and validated them using qRT-PCR. The qRT-PCR results showed that most of these selected genes had similar expression patterns with those identified in the RNA sequencing data (Fig. 8), which indicated that the transcriptome sequencing data had high repeatability and accuracy. The average of these correlation values was 0.613, and it was indicated that there was a high correlation between the results of RNA-seq and qRT-PCR. Meanwhile, 42.86% of these selected genes had a correlation value of over 0.81. The correlation coefficient was more than 0.933 in flavonoid synthesis gene *4CL*, *F3H*, and *ANR*. These results indicated that the relative levels of transcripts produced from the RNA-seq were in a good agreement with values obtained by qRT-PCR.

Discussion

Perilla as herb and oil plant was widely used in East Asia. Due to much more leaf color variations, and it was also used as an ornamental plant. Investigation of molecular

Table 4 The DEGs regulated chlorophyll metabolic pathway

No	Gene name	Unigene ID	Length	94-GG	272-GLP	103-GPP	357-PP
1	*glutamyl-tRNA synthetase* (*GluRS*)	CL1929.Contig3_All	2,483	2.18 ± 0.80	7.51 ± 0.59	7.12 ± 0.76	13.48 ± 0.95
2	*Glutamyl-tRNA reductase (GluTR/HEMA)*	CL6762.Contig1_All	1,437	33.94 ± 0.06	35.82 ± 3.05	68.24 ± 1.29	18.92 ± 3.64
		CL8793.Contig3_All	2,131	2.07 ± 0.41	2.70 ± 0.10	1.75 ± 0.13	0.89 ± 0.02
		Unigene15301_All	2,195	213.96 ± 4.82	236.18 ± 4.02	225.26 ± 0.43	118.00 ± 0.55
3	*Glutamate-1-semialdehyde 2,1-aminomutase(GSAAT)*	CL6883.Contig3_All	3,679	31.31 ± 1.29	26.91 ± 0.35	30.84 ± 0.90	17.67 ± 0.13
4	*5-aminolevulinate dehydratase(ALAD)*	Unigene9122_All	1,646	17.24 ± 0.01	29.80 ± 0.81	31.46 ± 1.14	61.15 ± 0.25
		Unigene15911_All	768	40.58 ± 0.40	2.72 ± 0.45	1.94 ± 1.24	25.64 ± 0.08
5	*Hydroxymethylbilane synthase(HEMC/HMBS)*	CL9339.Contig2_All	1,495	14.25 ± 0.47	9.15 ± 1.22	12.81 ± 0.72	13.28 ± 0.11
6	*uroporphyrinogen III synthase (HEMD/UROS)*	Unigene20647_All	1,228	36.17 ± 2.30	32.12 ± 0.32	39.04 ± 0.22	28.15 ± 0.32
7	*Uroporphyrinogen III decarboxylase (UROD)*	CL13981.Contig7_All	1,700	10.43 ± 0.51	6.88 ± 0.55	10.54 ± 1.22	1.89 ± 0.23
		CL4132.Contig1_All	2,331	9.29 ± 0.44	6.23 ± 1.01	10.73 ± 0.04	12.34 ± 0.20
8	*Coproporphyrinogen III oxidase (CPO)*	CL5607.Contig4_All	3,040	1.84 ± 0.14	1.59 ± 0.04	1.54 ± 0.16	0.62 ± 0.35
		Unigene12050_All	1,021	0.00 ± 0.00	0.19 ± 0.26	0.13 ± 0.18	9.59 ± 1.36
		CL2268.Contig3_All	1,401	31.75 ± 0.40	31.67 ± 0.40	30.71 ± 0.49	15.63 ± 0.26
9	*Protoporphyrinogen oxidase (PPOX)*	CL3522.Contig4_All	3,109	5.42 ± 0.18	4.83 ± 0.34	2.65 ± 0.58	0.75 ± 0.00
		CL1474.Contig27_All	2,601	3.33 ± 0.76	1.96 ± 0.01	2.38 ± 0.31	0.48 ± 0.30
		CL2458.Contig10_All	2,934	0.37 ± 0.11	0.70 ± 0.44	0.00 ± 0.00	0.35 ± 0.16
10	*Magnesium chelatase (MgCh)*	CL11069.Contig1_All	1,554	41.61 ± 2.96	23.65 ± 2.86	44.49 ± 2.45	47.46 ± 1.89
		CL9498.Contig1_All	4,986	259.57 ± 1.87	213.60 ± 0.74	217.16 ± 1.80	149.00 ± 3.68
		Unigene12797_All	2,580	45.46 ± 0.54	30.62 ± 0.21	37.88 ± 0.28	20.19 ± 0.53
11	*Magnesium protoporphyrin IX methyltransferase (CHLM)*	Unigene17397_All	3,320	21.20 ± 0.14	23.08 ± 0.17	29.24 ± 0.06	26.46 ± 0.00
12	*Magnesium-protoporphyrin IX monomethylester cyclase (CHL27)*	CL1169.Contig13_All	4,009	36.91 ± 3.45	29.77 ± 1.91	51.17 ± 0.21	57.09 ± 0.13
13	*Protochlorophyllide oxidoreductase (POR)*	Unigene673_All	1,396	2.79 ± 0.57	1.02 ± 0.26	1.44 ± 0.04	11.76 ± 0.95
		CL374.Contig6_All	2,832	0.23 ± 0.18	4.57 ± 0.61	3.16 ± 0.33	6.47 ± 0.30
14	*Divinyl reductase (DVR)*	CL1122.Contig2_All	1,969	12.16 ± 1.15	16.61 ± 1.79	15.16 ± 0.35	48.94 ± 1.17
		CL8802.Contig2_All	1,689	144.20 ± 0.66	79.99 ± 1.90	128.22 ± 2.87	77.22 ± 3.02
15	*Chlorophyll synthase (ChlG)*	CL5824.Contig3_All	1,631	24.74 ± 0.34	26.73 ± 2.98	31.35 ± 2.52	6.26 ± 0.02
16	*Chlorophyllide a oxygenase(CAO)*	CL2783.Contig1_All	2,272	8.01 ± 0.28	6.01 ± 0.23	9.33 ± 0.90	37.49 ± 1.07
		CL1364.Contig13_All	3,400	30.19 ± 1.94	26.51 ± 1.65	25.81 ± 0.13	25.83 ± 1.52
17	*Chlorophyll b reductase (CBR)*	CL2905.Contig6_All	2,440	1.51 ± 0.19	0.30 ± 0.01	0.32 ± 0.02	0.42 ± 0.04
		CL3043.Contig4_All	1,939	24.03 ± 0.73	4.70 ± 0.25	4.98 ± 0.76	2.88 ± 0.64
18	*Hydroxymethyl chlorophyll a reductase (HCAR)*	CL6020.Contig12_All	3,516	0.83 ± 0.33	1.61 ± 0.09	0.79 ± 0.11	0.86 ± 0.21
19	*Magnesium dechelatase (STAYGREEN/NON-YELLOWING (SGR/NYE) (MCS/SGR/NYE)*	CL5222.Contig3_All	1,368	58.38 ± 1.15	38.29 ± 0.62	0.18 ± 0.00	3.39 ± 0.57
		Unigene46613_All	1,023	12.35 ± 2.23	4.52 ± 0.83	37.06 ± 0.89	22.91 ± 0.05
		CL3099.Contig4_All	4,101	2.91 ± 0.32	4.21 ± 0.42	1.30 ± 0.27	1.78 ± 0.01
		CL3287.Contig1_All	1,673	10.74 ± 0.51	6.70 ± 1.01	8.69 ± 0.05	7.49 ± 0.12
		CL3709.Contig1_All	1,893	8.31 ± 0.08	5.67 ± 0.49	0.53 ± 0.08	0.90 ± 0.25
		CL6196.Contig1_All	1,261	23.65 ± 2.64	14.25 ± 0.59	0.68 ± 0.05	0.39 ± 0.21
		CL3865.Contig1_All	1,146	35.48 ± 0.43	20.87 ± 0.05	22.75 ± 1.70	19.16 ± 0.90

Table 4 (continued)

No	Gene name	Unigene ID	Length	94-GG	272-GLP	103-GPP	357-PP
20	*Pheophytinase (PPH)*	Unigene19598_All	1,907	4.55 ± 0.99	0.00 ± 0.00	5.14 ± 0.13	2.54 ± 0.37
		Unigene19602_All	1,579	5.19 ± 0.08	5.16 ± 0.43	5.75 ± 1.07	2.52 ± 0.06
		Unigene19603_All	1,634	6.45 ± 0.54	5.58 ± 1.04	4.93 ± 0.33	2.68 ± 0.59
		Unigene19608_All	2,239	0.00 ± 0.00	0.00 ± 0.00	0.00 ± 0.00	0.53 ± 0.08
		Unigene42901_All	920	0.00 ± 0.00	0.00 ± 0.00	3.79 ± 0.21	0.86 ± 0.32
		CL1060.Contig14_All	2,805	4.85 ± 0.42	4.82 ± 0.93	5.91 ± 0.15	20.42 ± 0.96
		CL11133.Contig1_All	3,167	42.26 ± 1.12	31.02 ± 1.87	29.02 ± 1.03	149.06 ± 1.39
		CL1652.Contig13_All	2,375	23.74 ± 1.37	17.51 ± 0.24	19.73 ± 0.58	7.87 ± 0.74
		CL2285.Contig5_All	1,200	5.47 ± 0.78	10.51 ± 1.62	5.43 ± 0.81	0.00 ± 0.00
21	*Pheophorbide a oxygenase (PAO)*	CL9496.Contig2_All	1,744	1.97 ± 0.19	4.19 ± 1.24	3.89 ± 0.84	12.83 ± 0.32
		CL1997.Contig6_All	1,573	2.57 ± 0.19	4.08 ± 0.33	3.50 ± 0.12	11.45 ± 0.87
		CL4104.Contig8_All	2,722	78.12 ± 2.96	99.38 ± 1.64	95.07 ± 1.00	154.49 ± 6.92
22	*Red chlorophyll catabolite reductase (RCCR)*	Unigene35253_All	1,187	0.10 ± 0.13	0.00 ± 0.00	0.00 ± 0.00	7.05 ± 1.10
		Unigene4771_All	2,897	0.45 ± 0.12	0.45 ± 0.06	0.64 ± 0.15	3.05 ± 0.25
		Unigene7171_All	1,358	24.11 ± 3.25	14.64 ± 1.46	27.43 ± 1.90	2.53 ± 1.99
		Unigene9514_All	1,853	26.22 ± 4.23	22.25 ± 0.03	5.67 ± 0.16	1.57 ± 0.20
		Unigene19354_All	1,471	3.13 ± 0.71	1.35 ± 1.10	10.44 ± 3.46	12.05 ± 2.53
		Unigene19360_All	1,399	7.80 ± 0.15	8.46 ± 2.28	15.80 ± 1.08	23.77 ± 4.54
		Unigene4575_All	698	2.82 ± 0.33	2.95 ± 0.33	0.59 ± 0.13	0.22 ± 0.03
23	*TIC55*	CL7170.Contig1_All	1,922	168.47 ± 1.60	149.52 ± 5.44	156.59 ± 1.68	128.71 ± 5.63

mechanism of leaf coloration might be applied for perilla breeding with desirable color. Previous studies showed that anthocyanin metabolism and related gene expression affected leaf color formation. However, only a few anthocyanin-related genes and transcription factors were identified in green and red perilla. The mechanism of leaf coloration should be further studied, especially, back leaf color variations. Generally, leaf color formation was determined three pigments including chlorophyll, carotenoid and flavonoid. However, the reported papers were not investigated the effect of chlorophyll, and carotenoid on leaf coloration. In our paper, four different perilla leaf colors were used as materials to compare the contents of three pigments and then identify leaf coloration genes by RNA-seq technology.

Difference analysis of three pigments in four perilla cultivars

Most of reports suggested that purple leaf has high contents of flavonoid/anthocyanin, and low content of carotenoid and chlorophyll (Lu et al. 2017; Shen et al. 2018). The red and green perilla forms were only regulated by anthocyanin production, but not that of other metabolites, such as inorganic anions, organic anions and amino acids (Yamazaki et al. 2003). However, it was found that both the total contents of chlorophyll and the content of chlorophyll *a* were all high in 357-PP, the completely purple leaf. Meanwhile the P_n was also high in M357-PP than those of the other three cultivars. The contents of anthocyanin and carotenoid were also largest in 357-PP, while anthocyanin was rich in 103-GPP with back purple leaf (Fig. 2). Thus, high contents of chlorophyll, carotenoid, and anthocyanin mixed together promote full purple leaf formation, while the content of anthocyanin was determined back leaf color formation. The correlation between the content of rosmarinic acid, and the total content of total anthocyanins was week (Deguchi and Ito 2020). The expression of *rosmarinic acid synthase* gene (CL13662.Contig2_All) was indeed low in high content of anthocyanins in green with dark purple and purple leaf in perilla. Green leaf might be accumulated much more rosmarinic acid in perilla. In fact, there was no difference of plant biological mass in four perilla cultivars (data was not shown). These results further suggested that perilla 357-PP with high P_n, and high contents of carotenoid, anthocyanin and flavonoid could be used as ornamental, edible, and medicinal plant.

Perilla leaf color regulated gene was identified by transcriptome sequencing

Saito et al. (1999) isolated anthocyanidin synthase (*ANS*) gene *2-oxoglutarate-dependent oxygenase* and verified its

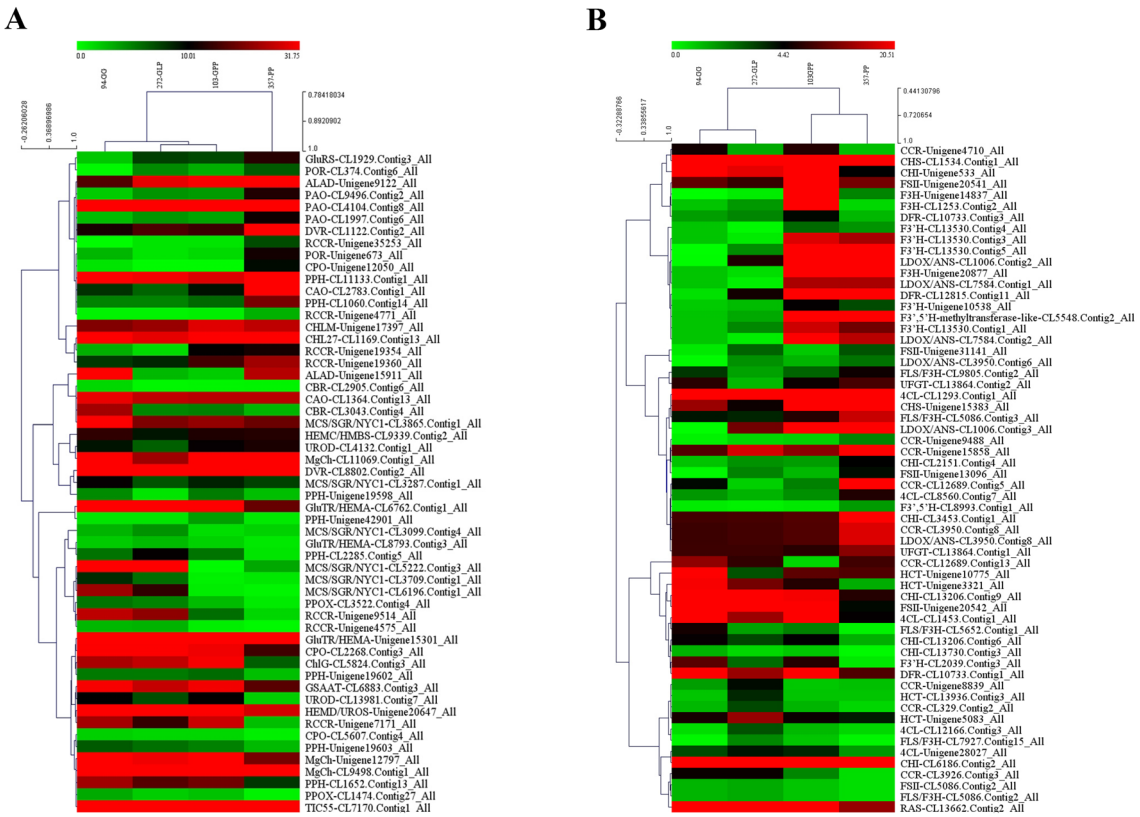

Fig. 6 The heatmap of the relative expression levels of the top highly differentially expressed genes (DEGs) in chlorophyll (A) and flavonoid (B) metabolism. The color scale (0.0–31.75) represents the expression levels of DEGs. The hierarchical clustering of unigenes and samples is shown in the dendrograms on the top and side of the heat map using the complete linkage approach

expression in green and red leaf perilla, for the first time. Then, Sompornpailin et al. (2002) isolated the gene *PFWD* (contained a WD repeat) controlled anthocyanin biosynthesis in perilla. Differential display of mRNA technology had been used to identify several genes encoding anthocyanin-biosynthetic enzymes and presumptive regulatory proteins (Yamazaki et al. 2003, 2008). Recently, transcriptome sequencing technology as a convenient tool was used to identify interested genes (Wang et al. 2018, 2019; Gao et al. 2020). In perilla, only a few papers were used RNA-seq to identify leaf color regulated genes, and the genes controlled back leaf color formations are still unknown.

Tong et al. (2015) used de novo assembly transcriptome sequencing generated 48,009 contigs with average length of 873 bp and a N50 length of 904 bp and identified the DEGs between *P. frutescens* (L.) var. *frutescens* and var. *crispa*. The unigenes number and average length in our work are larger than those reported studies in perilla (Tong et al. 2015; Jiang et al. 2020). Higher expression of *PfGST1* and *PfCHI1* was found in red perilla (Tong et al. 2015), and high expression of *CHS* gene enhanced the accumulation of flavonoids in red perilla (Jiang et al. 2020). They also deduced transcription factors including MYB, Myc-like, AP2/ERFs, WRKY, bHLH, MADS, WD40, and NACs, and flavonoid synthesized related genes including *PAL*, *C4H*, *CHS*, *F3H*, *F3'H*, *DFR*, *ANS*, *UFGT*, and *UGT75C1* involved in red leaf color formation (Tong et al. 2015; Jiang et al. 2020). The above flavonoid synthesized related genes together with *flavonol synthase* (*FLS*) were linked to fruit pigmentation in the olive and redness of leaf pigmentation in *Acer rubrum* (Chen et al. 2019; Iaria et al. 2016). *AmDFR* and *AmPAL1* were significant genes involved in the anthocyanin metabolic pathway and regulated leaf color change in *A. pictum* subsp. *Momo* (Ge et al. 2019). In *Paphiopedilum hirsutissimum*, *F3H* and *CHS* controlled essentially important steps in anthocyanin biosynthesis pathway and regulated flower color variation (Liu et al. 2018). It was deduced that those above genes related to anthocyanin synthesis may be realized green and purple leaf coloration in perilla.

In our work, the expression levels of these above genes were also found up-/down- regulated. According to the expression patterns of flavonoid related genes, it was found that the five genes, *F3'H*, *F3H*, *DFR*, *ANS*, and *F3',5'H* were the key genes control green and purple leaf coloration, and back leaf color change. Almost all of the five genes did not expressed in green leaf, and up-regulated expression during

Table 5 DEGs in flavonoid biosynthesis pathway

No	Gene name	Unigene ID	Length (bp)	94-GG	272-GLP	103-GPP	357-PP
1	*Phenyl alanineammonia lyase* (*PAL*)	CL13983.Contig3_All	2,507	24.24 ± 3.40	59.41 ± 2.64	16.58 ± 0.25	9.32 ± 0.62
		CL13983.Contig5_All	3,223	18.26 ± 0.44	31.96 ± 0.95	12.63 ± 1.41	7.29 ± 1.20
2	*Cinnamate 4-hydroxylase (C4H)*	Unigene27773_All	2,536	2.69 ± 0.83	5.37 ± 0.35	2.71 ± 0.43	1.18 ± 0.46
		CL6772.Contig5_All	1,727	10.73 ± 0.69	29.92 ± 1.87	3.03 ± 0.71	6.08 ± 1.87
		CL6772.Contig2_All	2,465	23.05 ± 1.58	33.07 ± 0.90	17.05 ± 0.25	13.40 ± 0.09
		Unigene14838_All	1,856	2.55 ± 0.27	6.14 ± 0.45	1.59 ± 0.52	1.44 ± 0.50
		Unigene14839_All	896	8.74 ± 1.45	26.01 ± 2.11	2.82 ± 0.37	5.00 ± 0.05
3	*p-coumarate 3 hydroxylase (C3H)*	CL11971.Contig9_All	1,874	43.59 ± 1.56	80.73 ± 0.45	35.85 ± 1.78	23.40 ± 0.78
4	*Caffeic O-methyltransferase (COMT)*	Unigene17835_All	1,561	69.91 ± 0.98	75.77 ± 4.86	68.58 ± 0.20	28.48 ± 0.77
		CL9808.Contig2_All	1,016	23.51 ± 0.61	57.27 ± 0.78	12.97 ± 0.86	24.58 ± 2.88
		Unigene20838_All	1,537	5.25 ± 0.18	12.69 ± 2.02	3.11 ± 0.11	6.54 ± 0.59
5	*4-coumarate-CoA Ligase (4CL)*	CL14054.Contig2_All	3,600	0.27 ± 0.04	0.59 ± 0.07	0.44 ± 0.18	1.61 ± 0.18
		CL1453.Contig1_All	3,246	40.35 ± 0.13	14.44 ± 0.83	20.75 ± 0.73	4.0.0476 ± 0.45
		CL8560.Contig7_All	1,706	1.79 ± 0.42	1.30 ± 0.11	1.91 ± 0.24	6.54 ± 0.99
		Unigene28027_All	1,797	3.11 ± 0.06	4.07 ± 0.21	3.75 ± 0.26	1.74 ± 0.35
		CL1293.Contig1_All	2,056	33.90 ± 1.46	24.04 ± 1.40	44.19 ± 1.57	81.74 ± 2.96
		CL12166.Contig3_All	3,110	0.58 ± 0.22	2.99 ± 0.28	1.21 ± 0.21	0.71 ± 0.01
		CL1293.Contig2_All	2,238	1.17 ± 1.00	28.11 ± 3.44	1.40 ± 0.00	1.30 ± 0.05
6	*Cynnamoyl CoA reductase (CCR)*	CL12689.Contig5_All	2,099	4.27 ± 0.24	0.83 ± 0.38	2.15 ± 0.27	20.82 ± 0.02
		CL12689.Contig13_All	2,192	13.61 ± 1.66	7.61 ± 0.06	0.70 ± 0.21	8.61 ± 0.04
		CL329.Contig2_All	2,386	1.22 ± 0.08	3.17 ± 0.30	1.28 ± 0.13	0.68 ± 0.04
		CL3926.Contig3_All	1,443	5.22 ± 0.12	5.17 ± 0.58	2.07 ± 0.11	0.58 ± 0.50
		CL9761.Contig1_All	9,154	0.08 ± 0.01	0.83 ± 0.16	0.21 ± 0.05	4.05 ± 0.01
		Unigene15858_All	1,624	9.69 ± 0.98	17.95 ± 1.43	13.27 ± 1.33	39.40 ± 0.76
		Unigene9488_All	1,991	0.24 ± 0.06	0.68 ± 0.06	0.82 ± 0.03	2.13 ± 0.22
		Unigene10450_All	1,381	4.58 ± 0.47	4.65 ± 0.04	9.61 ± 0.28	11.55 ± 0.20
		Unigene3767_All	3,532	1.33 ± 0.05	0.09 ± 0.00	1.46 ± 0.28	0.09 ± 0.06
		Unigene4710_All	774	5.64 ± 0.42	1.47 ± 0.23	6.82 ± 0.36	1.10 ± 0.07
		Unigene8839_All	4,673	1.68 ± 0.31	4.23 ± 0.46	0.95 ± 0.07	1.08 ± 0.01
		CL3950.Contig8_All	1,120	8.21 ± 1.70	8.76 ± 0.07	9.60 ± 0.54	18.42 ± 1.34
7	*Hydroxycinnamoyl transferase (HCT)*	CL13936.Contig3_All	1,834	0.00 ± 0.00	3.74 ± 0.37	0.00 ± 0.00	0.00 ± 0.00
		Unigene10775_All	2,903	38.97 ± 1.50	3.01 ± 0.06	10.30 ± 0.49	9.50 ± 0.87
		Unigene1890_All	1,630	0.34 ± 0.20	13.03 ± 1.00	0.30 ± 0.12	0.13 ± 0.02
		Unigene5083_All	3,253	5.98 ± 0.54	14.00 ± 0.65	5.19 ± 0.59	3.96 ± 0.45
		Unigene3321_All	1,073	20.25 ± 0.76	11.84 ± 0.28	6.77 ± 0.19	1.42 ± 0.21
		CL11508.Contig2_All	1,660	3.27 ± 0.35	5.87 ± 0.16	4.37 ± 0.19	13.95 ± 1.24
8	*Chalcone synthase (CHS)*	CL1534.Contig1_All	1,663	125.35 ± 7.76	38.89 ± 1.89	177.00 ± 12.99	48.87 ± 1.34
		Unigene15383_All	2,135	14.27 ± 0.93	5.28 ± 0.59	24.59 ± 0.75	49.96 ± 1.68
9	*Chalconeisomerase (CHI)*	CL13206.Contig6_All	1,113	4.88 ± 0.04	3.21 ± 0.41	4.56 ± 0.83	1.38 ± 0.01
		CL13206.Contig9_All	1,024	26.40 ± 0.26	20.51 ± 0.21	20.07 ± 1.40	6.79 ± 0.06
		CL13730.Contig3_All	1,617	1.29 ± 0.00	0.65 ± 0.04	0.94 ± 0.06	0.09 ± 0.04
		CL2151.Contig4_All	2,416	1.04 ± 0.28	1.86 ± 0.36	1.69 ± 0.22	4.54 ± 0.84
		CL3453.Contig1_All	2,322	8.70 ± 0.04	8.95 ± 0.92	9.72 ± 0.62	28.85 ± 1.46
		Unigene533_All	2,511	24.48 ± 1.62	19.11 ± 0.68	33.65 ± 0.26	4.61 ± 0.22
10	*Flavone synthase II (FSII)*	Unigene20542_All	1,856	34.45 ± 2.28	28.99 ± 4.13	26.76 ± 0.33	4.28 ± 0.01
		Unigene965_All	1,842	31.63 ± 2.47	14.99 ± 3.68	12.68 ± 0.86	5.58 ± 0.39
		CL7056.Contig3_All	1,376	2.36 ± 0.01	1.46 ± 0.28	5.52 ± 0.17	2.60 ± 0.16

Table 5 (continued)

No	Gene name	Unigene ID	Length (bp)	94-GG	272-GLP	103-GPP	357-PP
		Unigene20541_All	1,870	10.55 ± 1.16	7.96 ± 0.25	46.22 ± 0.11	11.92 ± 0.83
		Unigene13096_All	587	0.12 ± 0.17	2.14 ± 0.53	1.22 ± 0.52	4.21 ± 1.01
		Unigene31141_All	1,066	0.35 ± 0.08	2.69 ± 0.50	0.93 ± 0.16	2.98 ± 0.01
		CL13434.Contig1_All	1,988	1.54 ± 0.01	0.06 ± 0.03	3.45 ± 0.17	1.83 ± 0.53
		CL5086.Contig2_All	1,246	1.27 ± 0.12	1.45 ± 0.39	0.00 ± 0.00	0.58 ± 0.23
11	*Flavonol synthase (FLS)*	CL5086.Contig3_All	1,175	4.04 ± 0.40	3.80 ± 0.23	6.88 ± 0.96	17.21 ± 0.97
		CL7927.Contig15_All	813	0.13 ± 0.18	2.06 ± 0.58	0.00 ± 0.00	0.15 ± 0.21
		CL5086.Contig2_All	1,246	1.27 ± 0.12	1.45 ± 0.39	0.00 ± 0.00	0.58 ± 0.23
		CL3571.Contig5_All	927	42.25 ± 2.34	64.65 ± 3.32	105.77 ± 6.07	73.73 ± 0.03
		CL9805.Contig2_All	1,205	3.45 ± 0.83	1.61 ± 0.08	2.68 ± 0.23	5.46 ± 0.20
		CL5652.Contig1_All	1,286	5.79 ± 0.70	1.62 ± 0.11	2.20 ± 1.16	0.22 ± 0.30
		CL5652.Contig1_All	1,286	5.79 ± 0.70	1.62 ± 0.11	2.20 ± 1.16	0.22 ± 0.30
		Unigene6990_All	2,276	3.54 ± 0.10	2.86 ± 0.18	3.47 ± 0.38	0.52 ± 0.06
		CL3571.Contig5_All	927	42.25 ± 2.34	64.65 ± 3.32	105.77 ± 6.07	73.73 ± 0.03
		CL9805.Contig2_All	1,205	3.45 ± 0.83	1.61 ± 0.08	2.68 ± 0.23	5.46 ± 0.20
12	*Flavanone 3-hydroxylase (F3H)*	CL1253.Contig4_All	4,042	0.00 ± 0.00	0.22 ± 0.14	5.40 ± 0.52	0.39 ± 0.04
		CL1253.Contig2_All	2,980	0.00 ± 0.00	1.74 ± 0.01	22.82 ± 0.03	0.66 ± 0.21
		CL7927.Contig6_All	4,691	1.39 ± 0.18	3.44 ± 0.39	1.48 ± 0.16	0.90 ± 0.10
		Unigene14836_All	2,203	12.97 ± 0.84	3.19 ± 0.02	0.00 ± 0.00	1.31 ± 0.06
		Unigene14837_All	1,911	0.02 ± 0.02	0.32 ± 0.45	27.03 ± 1.20	2.11 ± 0.18
		Unigene20877_All	1,292	0.00 ± 0.00	0.56 ± 0.06	33.01 ± 0.15	34.57 ± 0.34
13	*Flavonol 3'-hydrogenase (F3'H)*	CL13530.Contig1_All	1,885	0.00 ± 0.00	2.04 ± 0.05	17.37 ± 1.26	11.60 ± 0.10
		CL13530.Contig3_All	1,962	0.00 ± 0.00	0.33 ± 0.05	18.49 ± 1.46	14.96 ± 1.57
		CL13530.Contig4_All	2,417	0.00 ± 0.00	0.10 ± 0.07	2.57 ± 0.31	1.84 ± 0.32
		CL13530.Contig5_All	1,976	0.02 ± 0.02	1.97 ± 0.09	26.77 ± 1.34	20.68 ± 0.82
		CL5548.Contig2_All	997	0.00 ± 0.00	1.49 ± 0.29	58.61 ± 2.93	33.01 ± 0.88
		Unigene10538_All	2,644	0.89 ± 0.03	1.15 ± 0.05	4.81 ± 0.03	3.11 ± 0.02
		Unigene11136_All	2,041	12.96 ± 1.06	7.30 ± 0.82	0.78 ± 0.02	0.23 ± 0.32
		CL2039.Contig3_All	8,445	10.12 ± 0.69	2.56 ± 0.06	6.87 ± 0.71	0.38 ± 0.04
		Unigene8486_All	2,369	1.94 ± 0.02	1.48 ± 0.27	0.82 ± 0.05	0.67 ± 0.08
14	*Flavonol 3'5'-hydrogenase (F3',5'H)*	CL8993.Contig1_All	1,594	0.34 ± 0.01	0.23 ± 0.11	0.35 ± 0.35	1.72 ± 0.18
	dihydroflavonol dihydroflavonol 4-reductase (DFR)	CL12815.Contig11_All	2,636	0.53 ± 0.20	5.67 ± 0.09	44.56 ± 1.01	24.08 ± 0.28
		CL10733.Contig1_All	1,513	26.85 ± 1.18	14.17 ± 0.10	20.71 ± 0.11	9.48 ± 0.91
		CL10733.Contig3_All	1,890	1.68 ± 0.06	2.07 ± 0.11	4.30 ± 1.18	1.22 ± 0.06
15	*Leucoanthocyanidin dioxygenase (LDOX/ANS)*	CL1006.Contig1_All	1,556	0.00 ± 0.00	6.55 ± 0.03	77.35 ± 0.26	29.13 ± 0.81
		CL1006.Contig2_All	1,626	0.04 ± 0.05	6.48 ± 0.23	178.33 ± 1.94	141.63 ± 1.03
		CL1006.Contig3_All	1,590	0.02 ± 0.03	11.58 ± 0.81	29.12 ± 1.61	56.57 ± 2.23
		CL7584.Contig1_All	1,309	0.00 ± 0.00	0.28 ± 0.18	15.21 ± 1.72	15.20 ± 2.06
		CL7584.Contig2_All	1,272	0.00 ± 0.00	0.31 ± 0.01	25.83 ± 1.66	16.12 ± 1.43
		CL3950.Contig7_All	1,431	1.30 ± 0.93	7.19 ± 1.03	4.49 ± 0.93	11.13 ± 0.74
		CL3950.Contig8_All	1,120	8.21 ± 1.70	8.76 ± 0.07	9.60 ± 0.54	18.42 ± 1.34
16	*UDP-glucose:anthocianidin:flavonoidglucosyltransferase (UFGT)*	CL13864.Contig2_All	1,621	7.09 ± 0.53	1.21 ± 0.08	5.25 ± 0.04	9.01 ± 0.94
		CL13864.Contig1_All	1,657	8.29 ± 0.13	8.29 ± 0.04	7.06 ± 0.21	13.18 ± 0.62
		Unigene5399_All	1,709	16.00 ± 2.71	19.39 ± 0.86	17.94 ± 0.71	10.65 ± 0.35
		CL7065.Contig2_All	1,667	2.85 ± 0.67	0.09 ± 0.12	6.09 ± 2.03	2.45 ± 0.06
		CL7065.Contig3_All	1,658	13.79 ± 0.01	0.90 ± 0.27	30.36 ± 0.40	7.82 ± 0.40

Table 5 (continued)

No	Gene name	Unigene ID	Length (bp)	94-GG	272-GLP	103-GPP	357-PP
17	*Anthocyanidinsynthase (ANS)*	CL3950.Contig1_All	1,210	43.78 ± 1.75	45.33 ± 1.79	25.61 ± 1.22	34.73 ± 1.68
		CL3950.Contig7_All	1,431	1.30 ± 0.93	7.19 ± 1.03	4.49 ± 0.93	11.13 ± 0.74
		CL3950.Contig2_All	1,231	1.32 ± 0.13	1.25 ± 0.13	0.42 ± 0.51	3.63 ± 1.01
		CL3950.Contig5_All	1,520	3.13 ± 0.12	0.00 ± 0.00	0.00 ± 0.00	0.00 ± 0.00
		CL3950.Contig6_All	1,402	0.07 ± 0.09	1.89 ± 0.16	1.28 ± 0.28	2.41 ± 0.25
		Unigene652_All	2,044	1.77 ± 0.12	2.98 ± 0.13	2.11 ± 0.13	0.62 ± 0.10
18	*Rosmarinic acid synthase (RAS)*	CL13662.Contig2_All	1,665	57.38 ± 3.85	86.89 ± 0.19	22.03 ± 2.23	14.04 ± 1.03
19	*UDP-glucoronosyl and UDP-glucosyl transferase (UGT88D7)*	Unigene12571_All	1,765	163.21 ± 0.70	143.22 ± 3.97	114.76 ± 3.61	36.67 ± 0.91
20	*Cytochrome P450 CYP98A78 (CYP98A78)*	CL306.Contig5_All	4,827	10.84 ± 0.40	19.51 ± 0.78	8.17 ± 0.05	5.56 ± 0.47

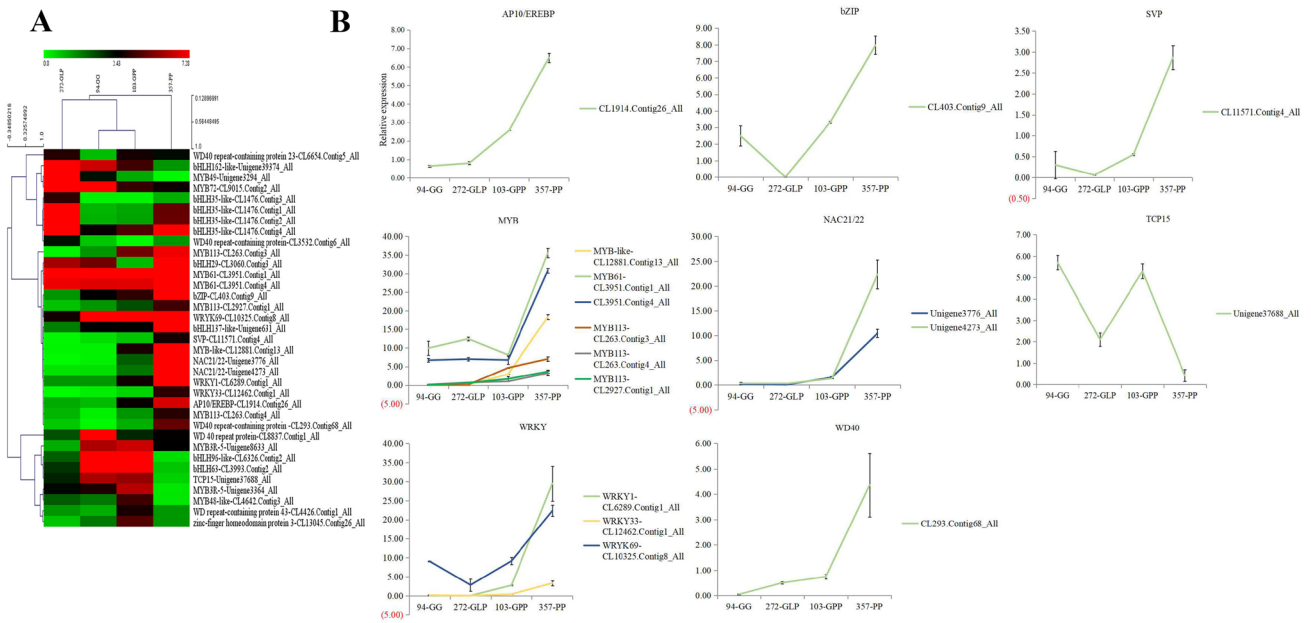

Fig. 7 The heatmap of the relative expression levels of the top highly differentially expressed genes (DEGs) (A), and expression patterns of the important DEGs according to FPKM analysis in four samples (B). The color scale (0.0–7.28) represents the expression levels of DEGs. The hierarchical clustering of unigenes and samples is shown in the dendrograms on the top and side of the heat map using the complete linkage approach

with back leaf color deepened. Especially, the gene *F3',5'H* specifically expressed in purple leaf 357-PP and back purple 103-GPP was found for the first time in perilla green and purple leaf, and it is very important gene induced delphinidin-3 glycoside synthesis. Therefore, delphinidin-3 glycoside is played role in perilla purple leaf coloration. In water lily (*Nymphaea colorata*), *F3',5'H* was controlled blue-petal formation (Zhang et al. 2020). This is further suggested that *F3',5'H* controlled purple leaf color formation in perilla. As a whole, according to the expression levels of flavonoid related genes suggested that 94-GG, 272-GLP, and 103-GPP can also synthesize flavones and flavonols, while anthocyanin synthesis was hampered in green leaf 94-GG.

Except of anthocyanin biosynthetic genes, the chlorophyll metabolic genes including *BoHEMA1*, *BoCRD1*, *BoPORC1*, *BoPORC2*, *BoCAO*, and *BoCLH1* were showed different expression levels in purple and white inner leaf pigmentation in ornamental cabbage (*Brassica oleracea* var. *acephala*) (Jin et al. 2018). Their results indicated that the purple inner leaves of purple ornamental cabbage result from a high level of anthocyanin biosynthesis, a high level of chlorophyll degradation and an extremely low level of chlorophyll biosynthesis (Jin et al. 2018). A total of 21 DEGs related to chlorophyll biosynthesis including *GluTR/HemA*, *HemC/HMBS*, *ChlD*, *ChlH*, *POR*, *ChlG* and *CAO* were up-regulated, and 10 to degradation containing *MCS/*

Table 6 Different expressed transcript factors in four perilla cultivars

No	Gene name	Unigene ID	Length (bp)	94-GG	272-GLP	103-GPP	357-PP
1	AP10/EREBP	CL1914.Contig26_All	3,675	0.64 ± 0.05	0.80 ± 0.08	2.57 ± 0.00	6.51 ± 0.25
2	bHLH35-like	CL1476.Contig1_All	1,641	0.69 ± 0.05	12.43 ± 0.59	0.83 ± 0.06	4.34 ± 0.11
		CL1476.Contig2_All	1,259	0.73 ± 0.02	13.15 ± 0.82	0.87 ± 0.33	4.45 ± 0.94
		CL1476.Contig3_All	3,896	0.12 ± 0.01	3.35 ± 0.10	0.11 ± 0.07	0.76 ± 0.12
		CL1476.Contig4_All	1,210	2.58 ± 0.28	25.97 ± 0.18	3.96 ± 0.59	11.75 ± 0.31
3	bHLH29	CL3060.Contig3_All	1,969	4.58 ± 0.35	5.55 ± 0.34	0.65 ± 0.08	20.36 ± 0.59
4	bHLH63	CL3993.Contig2_All	2,585	11.45 ± 0.29	1.94 ± 0.19	10.46 ± 0.86	0.55 ± 0.12
5	bHLH96-like	CL6326.Contig2_All	1,169	7.32 ± 0.95	1.53 ± 0.39	8.38 ± 1.96	0.31 ± 0.00
6	bHLH162-like	Unigene39374_All	565	6.33 ± 0.08	9.19 ± 2.35	3.67 ± 0.86	0.00 ± 0.00
7	bHLH137-like	Unigene631_All	2,674	2.42 ± 0.11	1.22 ± 0.23	2.42 ± 0.23	9.93 ± 1.18
		Unigene632_All	2,532	0.64 ± 0.21	0.00 ± 0.00	0.57 ± 0.28	1.85 ± 0.87
8	bZIP	CL403.Contig9_All	2,216	2.50 ± 0.60	0.00 ± 0.00	3.33 ± 0.06	7.98 ± 0.55
9	MADS-SVP	CL11571.Contig4_All	1,481	0.30 ± 0.33	0.06 ± 0.01	0.55 ± 0.02	2.87 ± 0.28
10	MYB-like	CL12881.Contig13_All	3,418	0.12 ± 0.00	0.09 ± 0.01	2.92 ± 0.01	18.36 ± 0.64
11	MYB3R-5	Unigene3364_All	9,287	3.00 ± 0.10	2.36 ± 0.37	5.92 ± 0.04	0.22 ± 0.02
		Unigene8633_All	3,902	5.73 ± 0.70	0.79 ± 0.24	6.34 ± 0.96	2.44 ± 1.39
12	MYB48-like	CL4642.Contig3_All	1,604	1.29 ± 0.13	1.57 ± 0.90	3.60 ± 0.02	0.23 ± 0.07
13	MYB49	Unigene3294_All	3,894	2.27 ± 0.23	7.28 ± 0.69	0.81 ± 0.08	0.06 ± 0.01
14	MYB61	CL3951.Contig1_All	1,557	9.94 ± 1.86	12.47 ± 0.52	8.14 ± 0.04	35.59 ± 1.27
		CL3951.Contig4_All	1,580	6.72 ± 0.51	7.01 ± 0.42	6.77 ± 1.07	30.85 ± 0.60
15	MYB72	CL9015.Contig2_All	934	10.63 ± 0.12	40.00 ± 0.23	3.44 ± 0.04	2.72 ± 0.30
16	MYB113	CL263.Contig3_All	870	0.00 ± 0.00	0.09 ± 0.12	4.65 ± 0.13	7.05 ± 0.64
		CL263.Contig4_All	1,818	0.13 ± 0.01	0.69 ± 0.11	1.00 ± 0.04	3.20 ± 0.67
		CL2927.Contig1_All	978	0.00 ± 0.00	0.57 ± 0.04	1.68 ± 0.65	3.63 ± 0.40
17	NAC21/22	Unigene3776_All	1,599	0.13 ± 0.04	0.04 ± 0.06	1.53 ± 0.20	10.45 ± 0.81
		Unigene4273_All	1,677	0.29 ± 0.24	0.25 ± 0.09	1.31 ± 0.01	22.39 ± 2.94
18	TCP15	Unigene37688_All	1,362	5.71 ± 0.34	2.10 ± 0.31	5.30 ± 0.35	0.42 ± 0.28
19	WRKY1	CL6289.Contig1_All	1,375	0.00 ± 0.00	0.00 ± 0.00	2.77 ± 0.13	29.50 ± 4.60
20	WRKY33	CL12462.Contig1_All	1,861	0.15 ± 0.13	0.02 ± 0.03	0.40 ± 0.04	3.31 ± 0.65
21	WRYK69	CL10325.Contig8_All	1,977	9.09 ± 0.11	2.80 ± 1.59	9.16 ± 0.92	22.36 ± 1.46
22	PRP4-like protein (contains WD40 repeats)	CL293.Contig68_All	1,882	0.05 ± 0.02	0.51 ± 0.05	0.75 ± 0.09	4.36 ± 1.26
23	autophagy-related protein 18b (contains WD40 repeats)	Unigene11308_All	3,223	0.45 ± 0.09	1.69 ± 0.06	1.76 ± 0.03	1.56 ± 0.41
24	WD40 repeat-containing protein 23	CL6654.Contig5_All	1,415	0.62 ± 0.47	3.17 ± 0.08	2.85 ± 0.95	2.33 ± 0.58
25	WD40 repeat-containing protein	CL3532.Contig6_All	3,410	0.53 ± 0.38	2.26 ± 0.05	0.02 ± 0.02	0.00 ± 0.00
	WD40 repeat-containing protein	CL6654.Contig3_All	1,543	1.13 ± 0.93	0.00 ± 0.00	0.00 ± 0.00	0.11 ± 0.16
	WD 40 repeat protein	CL8837.Contig1_All	697	11.53 ± 0.87	1.64 ± 0.67	2.05 ± 0.53	2.56 ± 0.74
26	WD repeat-containing protein 43	CL4426.Contig1_All	1,267	0.77 ± 0.21	0.00 ± 0.00	2.94 ± 0.43	0.00 ± 0.00
27	WD repeat domain-containing protein 83	Unigene23099_All	2,401	3.20 ± 0.39	0.12 ± 0.07	1.29 ± 0.30	1.27 ± 0.11
28	zinc-finger homeodomain protein 3	CL13045.Contig26_All	2,855	1.27 ± 0.20	0.56 ± 0.25	4.04 ± 0.36	0.00 ± 0.00

SGR/NYC1, and *PAO* were down-regulated in green leaf color of *Pennisetum setaceum* 'Rubrum', compared with those in purple leaf (Zhu et al. 2020). Therefore, in the last stage of chlorophyll biosynthesis and chlorophyll degradation were essentially steps for leaf color formation (from green to purple). However, from purple color to green color change, up-regulated *Glu-TR* expression induced chlorophyll accumulation in bicolor leaf of ornamental kale (Ren et al. 2019). In different perilla leaves with four kinds of colors, the expression patterns of *CHLM*, *CHL27*, *POR*, *DVR*, *CAO*, and *HCAR* (in the last stage of chlorophyll biosynthesis), and *NYC1*, and *PAO* (chlorophyll degradation) were consistent with those of *Pennisetum setaceum* 'Rubrum'. These

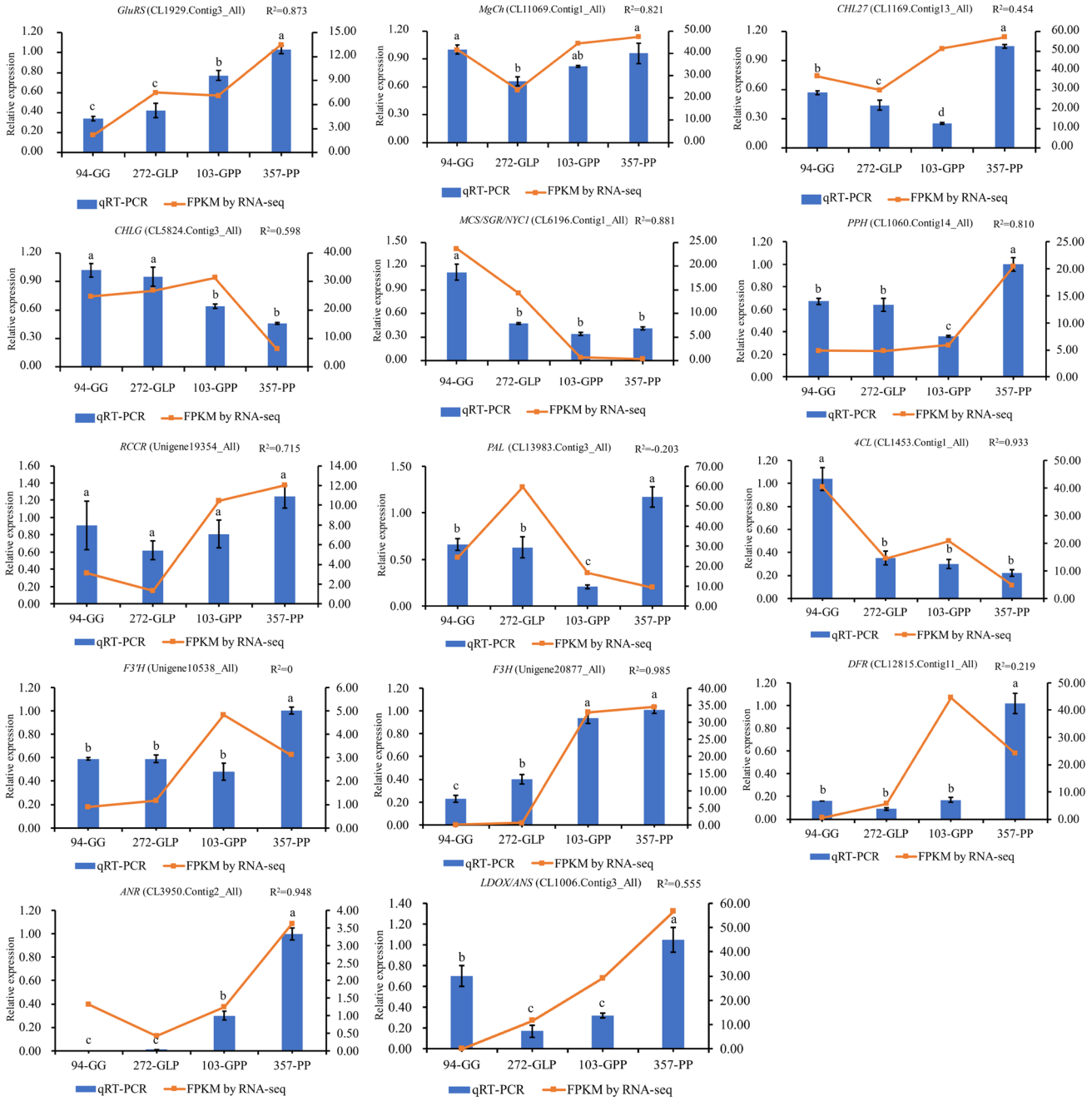

Fig. 8 The expression patterns of the 14 randomly selected DEGs confirmation of RNA-seq data by qRT-PCR analysis

genes were related to green and purple leaf color formation in perilla.

Carotenoids are one of the three largest classes of pigments and are also colorants that range from colorless to yellow, orange, and red, with variations reflected in many species (Chen et al. 2019). The contents of chlorophyll, anthocyanin, and carotenoid together determined leaf pigmentation in *A. rubrum* (Chen et al. 2019). Leaf pigmentation from green to red and then yellow, contents of carotenoids was down-regulated and the rate-limiting enzyme PSY were highly concentrated in yellow and green leaf. In perilla, *PSY2* was highly expressed in green leaf 94-GG. However, DEGs, *zeaxanthin epoxidase* (*ZEP*) and *violaxanthin de-epoxidase* (*VDE*) at the downstream stage of carotenoid biosynthetic pathway were up- and down-regulated expression, respectively, in purple leaf 357-GG, and the two genes promoted violaxanthin accumulation. High quantities of carotenoids accumulated in 357-PP caused

purple leaf color formation. The down-up-down expression patterns of *15-cis-zeta-carotene isomerase* (*ZIISO*), *beta-carotene isomerase D27*, *15-cis-zeta-carotene isomerase*, *cytochrome P450 CYP97A41* (*CYP97A*) suggested that more lutein accumulation in green leaf 94-GG.

Transcription factors regulated perilla leaf coloration

Among various transcription factors, MYB and bHLH are most significant regulators of flower or leaf variations, and MYB and bHLH transcription factors were also identified in our work. R2R3-type MYB transcription factors forming MYB-bHLH-WD10 complex regulate anthocyanin biosynthesis (Liu et al. 2018). R2R3 MYB transcript factor, *MYB113*, and *MYB110a* controls purple spot formation at the base of flower petals, and flower petal color in tetraploid cotton, and kiwifruit, respectively (Zhang et al. 2021; Abid et al. 2022). Zhang et al. (2021) found *MYB113* played the pivotal role in perilla leaf coloration. The *MYB113* was also identified in our work, and *MYB-like* gene (CL12881.Contig13_All) had similar expression pattern with *MYB113*. It was deduced that *MYB113* and *MYB-like* gene ((CL12881.Contig13_All) were two important MYB transcript factors controlled perilla leaf coloration. The yeast two-hybrid system showed PFWD strong interacted with MYB-like protein and finally, enhanced anthocyanin production in perilla (Sompornpailin et al. 2002). The hierarchical clustering thermogram showed that *bHLH29* (CL3060.Contig3_All) and *bHLH137-like* (Unigene631_All) were clustered in the same branch with *MYB113*, and they may be formed MYB-bHLH-WD10 complex to regulated anthocyanin synthesis (Fig. 7).

In apple, the expression level of the NAC (no apical meristem) transcription factor, *MdNAC52*, which controlled *MdMYB9* and *MdMYB11* expression, was increased during apple coloration, and overexpressed *MdNAC52* gene promoted anthocyanin accumulation (Sun et al. 2019). In our work, the *NAC21/22* (Unigene3776_All) was also showed high expression in purple perilla leaf of 357-PP, and could be advanced anthocyanin accumulation in purple leaf. In kiwifruit, overexpression of the kiwifruit *SVP3* gene interfered with the expression of *MYB110a*, which encodes the key anthocyanin biosynthetic step, *F3GT1*, and finally suppressed anthocyanin biosynthesis in petals (Wu et al. 2014). Unlike kiwifruit *SVP3*, the *SVP* gene may be a positive regulator of anthocyanin synthesis. The bZIP transcription factor *HY5* could directly recognize and bind the promoter of *chalcone synthase 1*, *chalcone synthase 2*, and *dihydroflavonol 4-reductase* to induce anthocyanin biosynthesis in tomato (Liu et al. 2018). The *bZIP* also showed high expression in purple perilla leaves, and it might be promoted anthocyanin accumulation. The *PbWRKY75* promotes anthocyanin synthesis by activating *PbDFR*, *PbUFGT*, and *PbMYB10a* in pear (Cong et al. 2018). Like pear *WRKY75*, *WRKY1* (CL6289.Contig1_All) and *WRKY33* (CL12462.Contig1_All) all advanced anthocyanin synthesis. TCP15 attenuates anthocyanin accumulation after short time exposition to high light intensity (Ivana et al. 2016), which was consistent with our result. Thus, *TCP15* was another important transcription factor in regulating perilla leaf coloration. According to expression pattern of *AP10/EREBP*, it was a positive regulator of anthocyanin synthesis.

The probable regulated scheme of perilla leaf coloration

The completely purple leaf color formation was determined by the high contents of chlorophyll, carotenoid, flavonoid, and anthocyanin, while different deepened back leaf color was caused by anthocyanin accumulation (Fig. 9). The contents of these pigments were caused by expression levels of these important genes of pigment synthesis and metabolism. In purple leaf, chlorophyll synthesis was lower than that of green leaf. However, down-regulated expression of *MCS/SGR/NYC1NYC1* may be delayed initial cholorophyll degradation. The initially high content of chlorophyll kept high photosynthesis rate of 357-PP. However, chlorophyll degradation was fast throughout up-regulation of chlorophyll degradation genes *PPH*, *PAO*, and *RCCR* at last. The chlorophyll degradation was unmasked purple color of 357-PP. The actively accumulated carotenoid by high expression of the regulator gene *ZEP* may be took part in light harvesting and leaf coloration in 357-PP. Much more expression of *F3'H*, *F3',5'H*, *F3H*, *DFR*, and *LDOX/ANS* promoted anthocyanin accumulation, and induced purple leaf color and back leaf purple color formation. Transcription factor genes, *MYB113*, *MYB-like*, *bHLH29*, *bHLH137-like*, *NAC21/22*, *WRKY1*, *WRKY33*, *SVP*, and *bZIP*, and *TCP15* played roles in anthocyanin accumulation, together with the above flavonoid synthesized related genes. According to previous study, it was deduced that *TCP15* negatively regulated anthocyanin accumulation, and leaf prolonged light exposure affected expression level of *TCP15*, and finally caused the lower surface of perilla leaf purple color formation.

Conclusions

In this study, comparative transcriptome was used to explore genes regulated green, purple and biocolor leaf in perilla. The differences of chlorophyll synthesis, and degradation, carotenoid accumulation, and anthocyanin synthesis in leaves with different colors caused perilla leaf coloration.

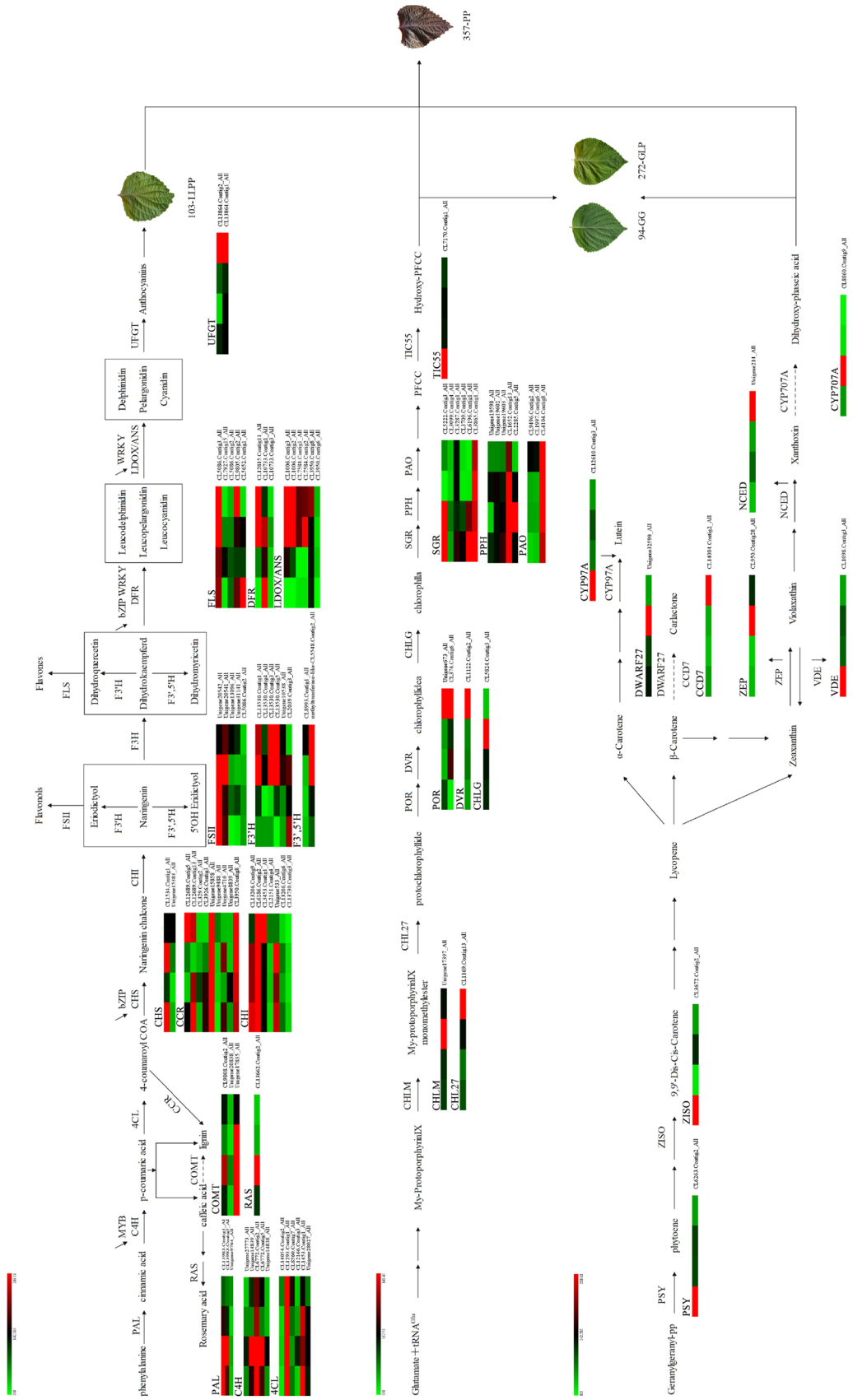

Fig. 9 The postulate scheme of leaf color variations regulated by anthocyanin, chlorophyll, and carotenoid, in perilla. Heatmaps were generated using long2FC based on FPKM values and the color scale (0.0–233.13) represents the expression levels of DEGs

These genes *CHLM*, *CHL27*, *POR*, *DVR*, *CAO*, *NYC1*, *PPH*, *PAO*, and *RCCR* controlled chlorophyll synthesis and degradation. The up- and down-regulated *ZEP* and *VDE* expression at the downstream stage of carotenoid biosynthetic pathway induced xanthoxin accumulation. The up-regulation of anthocyanin biosynthesis genes *F3'H*, *F3',5'H*, *F3H*, *DFR*, and *LDOX/ANS* is probably leading to perllia full purple leaf and back leaf coloration, while transcription factors MYB113, MYB-like, bHLH29, bHLH137-like, NAC21/22, WRKY1, WRKY33, SVP, and bZIP, and TCP15 together with the above genes might positively and negatively regulated anthocyanin synthesis, respectively. Further functional characterization of these identified genes could be further deciphered the mechanism of perilla leaf coloration.

Supplementary Information The online version contains supplementary material available at https://doi.org/10.1007/s11103-023-01342-8.

Acknowledgements We thank LetPub (www.letpub.com) for its linguistic assistance during the preparation of this manuscript. Meanwhile, we would like to thank Prof. Lijun Wang and Qi Shen for kindly providing the preilla seeds for us.

Authors' contributions SW, and XZ conceived and designed the experiments, and obtained the funding.SW, XL, YZ, JL conducted the experiment and contributed to the investigation. JX analyzed part transcriptome data. SW wrote the manuscript. MT provided suggestions and comments for the manuscript. All authors read and approved the final manuscript.

Funding The work was supported by China Agriculture Research System (CARS-21), China Association for Science and Technology Foundation for Young Scholars (2015QRNC001), and the Agricultural Science and Technology Innovation Program (ASTIP) of the Chinese Academy of Agricultural Sciences (CAAS-ASTIPIVFCAAS). The funding bodies have no role in the study design, data collection and analysis, decision to publish, or preparation of the manuscript.

Data availability The sequenced datasets presented in this study can be found in online repositories (https://www.ncbi.nlm.nih.gov). These data will remain private until the related manuscript has been accepted.

Declarations

Competing interest The authors declare that they have no competing interests.

References

Abid MA, Wei Y, Meng Z, Wang Y, Ye Y, Wang Y, He H, Zhou Q, Li Y, Wang P, Li X (2022) Increasing floral visitation and hybrid seed production mediated by beauty mark in *Gossypium hirsutum*. Plant Biotechnol J 20(7):1274–1284

Altschul SF, Gish W, Miller W, Myers EW, Lipman DJ (1990) Basic local alignment search tool. J Mol Biol 215(3):403–410. https://doi.org/10.1016/S0022-2836(05)80360-2

Benjamini Y, Yekutieli D (2011) The control of the false discovery rate in multiple testing under dependency. Ann Stat 29:1165–1188. https://doi.org/10.1214/aos/1013699998

Chen Z, Lu X, Xuan Y, Tang F, Wang J, Shi D et al (2019) Transcriptome analysis based on a combination of sequencing platforms provides insights into leaf pigmentation in *Acer rubrum*. BMC Plant Biol 19:240. https://doi.org/10.1186/s12870-019-1850-7

Conesa A, Gotz S, Garcia-Gomez JM, Terol J, Talon M, Robles M (2005) Blast2GO: a universal tool for annotation, visualization and analysis in functional genomics research. Bioinformatics 21:3674–3676. https://doi.org/10.1093/bioinformatics/bti610

Cong L, Qu Y, Sha G, Zhang S, Ma Y, Chen M et al (2021) *PbWRKY75* promotes anthocyanin synthesis by activating *PbDFR*, *PbUFGT*, and *PbMYB10b* in pear. Physiol Plant 173:1841–1849. https://doi.org/10.1111/ppl.13525

Deguchi Y, Ito M (2020) Caffeic acid and rosmarinic acid contents in genus *Perilla*. J Nat Med 74:834–839. https://doi.org/10.1007/s11418-020-01418-5

Gaihre YR, Tsuge K, Hamajima H, Nagata Y, Yanagita T (2021) The contents of polyphenols in *Perilla frutescens* (L.) Britton var. *frutescens* (Egoma) leaves are determined by vegetative stage, spatial leaf position, and timing of harvesting during the day. J Oleo Sci 70:855–859. https://doi.org/10.5650/jos.ess20291

Gao J, Xue J, Xue Y, Liu R, Ren X, Wang S et al (2020) Transcriptome sequencing and identification of key callus browning-related genes from petiole callus of tree peony (*Paeonia suffruticosa* cv. Kao) cultured on media with three browning inhibitors. Plant Physiol Bioch 149:36–49. https://doi.org/10.1016/j.plaphy.2020.01.029

Ge W, Wang X, Li J, Zhu W, Cui J, Zhang K (2019) Regulatory mechanisms of leaf color change in *Acer pictum* subsp. *mono*. Genome 62:793–805. https://doi.org/10.1139/gen-2019-0115

Grabherr MG, Haas BJ, Yassour M, Levin JZ, Thompson DA, Amit I et al (2011) Full-length transcriptome assembly from RNA-Seq data without a reference genome. Nat Biotechnol 29:644–652. https://doi.org/10.1038/nbt.1883

Iaria, D.L., Chiappetta, A., and Muzzalupo, I.A. (2016). De novo transcriptomic approach to identify flavonoids and anthocyanins "Switch-Off" in Olive (*Olea europaea* L.) drupes at different stages of maturation. Front Plant Sci 6:1246. https://doi.org/10.3389/fpls.2015.01246

Ivana L, Viola A, Camoirano D, H., and Gonzalez. (2016) Redox-dependent modulation of anthocyanin biosynthesis by the TCP transcription factor TCP15 during exposure to high light intensity conditions in *Arabidopsis*. Plant Physiol 170:74–85. https://doi.org/10.1104/pp.15.01016

Ivanov LA, Ronzhina DA, Yudina PK, Zolotareva NV, Kalashnikova IV, Ivanova LA (2020) Seasonal dynamics of the chlorophyll and carotenoid content in the leaves of steppe and forest plants on species and community level. Russian J Plant Physiol 67:453–462. https://doi.org/10.1134/S1021443720030115

Jiang T, Guo K, Liu L, Tian W, Xie X, Wen S et al (2020) Integrated transcriptomic and metabolomic data reveal the flavonoid biosynthesis metabolic pathway in *Perilla frutescens* (L.) leaves. Sci Rep 10:16207. https://doi.org/10.1038/s41598-020-73274-y

Jin SW, Rahim MA, Afrin KS, Park JI, Kang JG, Nou IS (2018) Transcriptome profiling of two contrasting ornamental cabbage (*Brassica oleracea* var. *acephala*) lines provides insights into purple and white inner leaf pigmentation. BMC Genomics 19:797. https://doi.org/10.1186/s12864-018-5199-3

Kwak Y, Ju J (2015) Inhibitory activities of *Perilla frutescens* britton leaf extract against the growth, migration, and adhesion of human cancer cells. Nutr Res Pract 9:11–16. https://doi.org/10.4162/nrp.2015.9.1.11

Li X, Fan J, Luo S, Yin L, Liao H, Cui X et al (2021) Comparative transcriptome analysis identified important genes and regulatory pathways for flower color variation in *Paphiopedilum hirsutissimum*. BMC Plant Biol 21:495. https://doi.org/10.1186/s12870-021-03256-3

Liu CC, Chi C, Jin LJ, Zhu J, Yu JQ, Zhou YH (2018) The bZip transcription factor *HY5* mediates *CRY1a*-induced anthocyanin biosynthesis in tomato. Plant Cell Environ 41:1762–1775. https://doi.org/10.1111/pce.13171

Lohse M, Bolger AM, Nagel A, Fernie AR, Lunn JE, Stitt M et al (2012) RobiNA: a user-friendly, integrated software solution for RNA-Seq-based transcriptomics. Nucleic Acids Res 40:W622–W627. https://doi.org/10.1093/nar/gks540

Lu N, Bernardo EL, Tippayadarapanich C, Takagaki M, Kagawa N, Yamori W (2017) Growth and accumulation of secondary metabolites in Perilla as affected by photosynthetic photon flux density and electrical conductivity of the nutrient solution. Front Plant Sci 8:708. https://doi.org/10.3389/fpls.2017.00708

Matvieieva N, Drobot K, Duplij V, Ratushniak Y, Shakhovsky A, Kyrpa-Nesmiian T et al (2019) Flavonoid content and antioxidant activity of *artemisia vulgaris* L. "hairy" roots. Prep Biochem Biotechnol 49:82–87. https://doi.org/10.1080/10826068.2018.1536994

McGuire RG (2019) Reporting of objective color measurements. HortScience 27:1254–1255. https://doi.org/10.1016/0304-4238(93)90147-I

Miki S, Wada KC, Takeno K (2015) A possible role of an anthocyanin filter in low-intensity light stress-induced flowering in *Perilla frutescens* var. *crispa*. J Plant Physiol 175:157–162. https://doi.org/10.1016/j.jplph.2014.12.002

Nakajima A, Yamamoto Y, Yoshinaka N, Namba M, Matsuo H, Okuyama T et al (2015) A new flavanone and other flavonoids from green Perilla leaf extract inhibit nitric oxide production in interleukin 1β-treated hepatocytes. Biosci Biotechnol Biochem 79:138–146. https://doi.org/10.1080/09168451.2014.962474

Rabino I, Mancinelli AL (1986) Light, temperature, and anthocyanin production. Plant Physiol 81:922–924. https://doi.org/10.1104/pp.81.3.922

Ren J, Liu Z, Chen W, Xu H, Feng H (2019) Anthocyanin degrading and chlorophyll accumulation lead to the formation of bicolor leaf in ornamental Kale. Int J Mol Sci 20:603. https://doi.org/10.3390/ijms20030603

Saito K, Kobayashi M, Gong ZZ, Tanaka Y, Yamazaki M (1999) Direct evidence for anthocyanidin synthase as a 2-oxoglutarate-dependent oxygenase: molecular cloning and functional expression of cDNA from a red forma of *Perilla frutescens*. Plant J 17:181–189. https://doi.org/10.1046/j.1365-313x.1999.00365.x

Shen J, Zou Z, Zhang X, Zhou L, Wang Y, Fang W et al (2018) Metabolic analyses reveal different mechanisms of leaf color change in two purple-leaf tea plant (*Camellia sinensis* L.) cultivars. Hort Res 5:7. https://doi.org/10.1038/s41438-017-0010-1

Sompornpailin K, Makita Y, Yamazaki M, Saito KA (2002) WD-repeat-containing putative regulatory protein in anthocyanin biosynthesis in *Perilla frutescens*. Plant Mol Biol 50:485–495. https://doi.org/10.1023/a:1019850921627

Sun Q, Jiang S, Zhang T, Xu H, Fang H, Zhang J et al (2019) Apple NAC transcription factor *MdNAC52* regulates biosynthesis of anthocyanin and proanthocyanidin through *MdMYB9* and *MdMYB11*. Plant Sci 289:110286. https://doi.org/10.1016/j.plantsci.2019.110286

Tang WF, Tsai HP, Chang YH, Chang TY, Hsieh CF, Lin CY et al (2021) Perilla (*Perilla frutescens*) leaf extract inhibits SARS-CoV-2 via direct virus inactivation. J Biomed 44:293–303. https://doi.org/10.1016/j.bj.2021.01.005

Tong W, Kwon SJ, Lee J, Choi IY, Park YJ, Choi SH et al (2015) Gene set by de novo assembly of Perilla species and expression profiling between *P-frutescens* (L.) var. *frutescens* and var. *crispa*. Gene 559:155–163. https://doi.org/10.1016/j.gene.2015.01.028

Voss DH (1992) Relating colorimeter measurement of plant color to the royal horticultural society colour chart. HortScience 27:1256–1260. https://doi.org/10.21273/HORTSCI.27.12.1256

Wang SL, Shen XX, Ge P, Li J, Subburaj S, Li XH et al (2012) Molecular characterization and dynamic expression patterns of two types of γ-gliadin genes from *Aegilops* and *Triticum* species. Theor Appl Genet 125:1371–1384. https://doi.org/10.1007/s00122-012-1917-4

Wang J, Guo M, Li Y, Wu R, Zhang K (2018) High-throughput transcriptome sequencing reveals the role of anthocyanin metabolism in *Begonia semperflorens* under high light stress. Photochem Photobiol 94:105–114. https://doi.org/10.1111/php.12813

Wang S, Gao J, Xue J, Xue Y, Li D, Guan Y et al (2019) De novo sequencing of tree peony (*Paeonia suffruticosa*) transcriptome to identify critical genes involved in flowering and floral organ development. BMC Genomics 20:572. https://doi.org/10.1186/s12864-019-5857-0

Wang S, Ren X, Xue J, Xue Y, Zhang X (2020a) Molecular characterization and expression analysis of the *SQUAMOSA PROMOTER BINDING PROTEIN-LIKE* gene family in *Paeonia suffruticosa*. Plant Cell Rep 39:1425–1441. https://doi.org/10.1007/s00299-020-02573-5

Wang ZX, Lin QQ, Tu ZC, Zhang L (2020b) The influence of in vitro gastrointestinal digestion on the *Perilla frutescens* leaf extract: changes in the active compounds and bioactivities. J Food Biochem. https://doi.org/10.1111/jfbc.13530

Wu R, Wang T, McGie T, Voogd C, Allan AC, Hellens RP et al (2014) Overexpression of the kiwifruit *SVP3* gene affects reproductive development and suppresses anthocyanin biosynthesis in petals, but has no effect on vegetative growth, dormancy, or flowering time. J Exp Bot 65:4985–4995. https://doi.org/10.1093/jxb/eru264

Yamazaki M, Nakajima J, Yamanashi M, Sugiyama M, Makita Y, Springob K et al (2003) Metabolomics and differential gene expression in anthocyanin chemo-varietal forms of *Perilla frutescens*. Phytochemistry 62:987–995. https://doi.org/10.1016/s0031-9422(02)00721-5

Yamazaki M, Shibata M, Nishiyama Y, Springob K, Kitayama M, Shimada N et al (2008) Differential gene expression profiles of red and green forms of *Perilla frutescens* leading to comprehensive identification of anthocyanin biosynthetic genes. FEBS J 275:3494–3502. https://doi.org/10.1111/j.1742-4658.2008.06496.x

Zhang L (2021) *Perilla frutescens* leaf extract and fractions: polyphenol composition, antioxidant, enzymes (α-Glucosidase, Acetylcholinesterase, and Tyrosinase) inhibitory, anticancer, and antidiabetic activities. Foods 10:315. https://doi.org/10.3390/foods10020315

Zhang L, Chen F, Zhang X, Li Z, Zhao Y, Lohaus R et al (2020) The water lily genome and the early evolution of flowering plants. Nature 577:79–84. https://doi.org/10.1038/s41586-019-1852-5

Zhang Y, Shen Q, Leng L, Zhang D, Chen S, Shi Y et al (2021) Incipient diploidization of the medicinal plant Perilla within 10,000 years. Nat Commun 12:5508. https://doi.org/10.1038/s41467-021-25681-6

Zheng YF, Li DY, Sun J, Cheng JM, Chai C, Zhang L et al (2020) Comprehensive comparison of two color varieties of *Perillae folium* using rapid resolution liquid chromatography coupled with quadruple-time-of-flight mass spectrometry (RRLC-Q/TOF-MS)-based metabolic profile and in vivo/in vitro anti-oxidative activity. J Agric Food Chem 68:14684–14697. https://doi.org/10.1021/acs.jafc.0c05407

Zhu T, Wang X, Xu Z, Xu J, Li R, Liu N et al (2020) Screening of key genes responsible for *Pennisetum setaceum* "Rubrum" leaf color using transcriptome sequencing. PLoS ONE 15:e0242618. https://doi.org/10.1371/journal.pone.0242618